
**BIOTECHNOLOGY AS A TOOL FOR
UNDERSTANDING BIOLOGICAL PROCESSES.
TWO CASE STUDIES: PED-PLD1
INTERACTION AND *pote* EXPRESSION.**

Dott.ssa Francesca Viparelli

Dottorato in Scienze Biotecnologiche – XIX ciclo
Indirizzo Biotecnologie Molecolari
Università di Napoli Federico II



Dottorato in Scienze Biotecnologiche – XIX ciclo
Indirizzo Biotecnologie Molecolari
Università di Napoli Federico II



**BIOTECHNOLOGY AS A TOOL FOR
UNDERSTANDING BIOLOGICAL PROCESSES.
TWO CASE STUDIES: PED-PLD1
INTERACTION AND *pote* EXPRESSION.**

Dott.ssa Francesca Viparelli

Dottoranda: Dott.ssa Francesca Viparelli

Relatore: Prof. Ettore Benedetti
Correlatore: Dr. Menotti Ruvo

Coordinatore: Prof. Gennaro Marino

Ai miei genitori

INDEX

RIASSUNTO	1
SUMMARY	6
1. INTRODUCTION	7
1.1 Recombinant protein expression	7
1.2 PED-PLD1	7
1.3 Real-time BIA	10
1.4 POTE	12
1.5 Lentiviral expression system	13
1.6 Aim of thesis	14
2. RESULTS	15
2.1 PED-D4 interaction	15
2.1.1 PED cloning, expression and purification	15
2.1.2 PED characterization	16
2.1.2a Mass spectrometry	16
2.1.2b 3-dimensional structure	17
2.1.3 D4 cloning, expression and purification	19
2.1.4 D4 dimerization	21
2.1.5 PED-D4 binding	22
2.1.5a ELISA assays	22
2.1.5b: Surface Plasmon Resonance	23
2.1.6 Competition assay	24
2.2 POTE 2γ	27
2.2.1 Lentivirus production	27
2.2.2 POTE 2γ expression in MCF10A cells	28
2.2.3 RNA interference	29
3. CONCLUSIONS	31
4. EXPERIMENTAL PROCEDURES	33
4.1 Materials and instruments	33
4.2 PED and D4 cloning	33
4.3 PED and D4 expression screening	33
4.4 PED purification	34
4.5 D4 purification	34
4.6 PED and D4 characterization	35
4.7 SUPERDEX75 10/300 GL and SUPERDEX200 HT 10/30 calibrations	36
4.8 ELISA assays	37
4.9 PED coating on sensor surface	37
4.10 Preparation of PED peptides	37
4.11 HEK293T cell transfection with pLenti6/V5-GW/lacZ	38
4.12 X-gal staining	38
4.13 Crystal violet staining for Blasticidin resistant colonies	38
4.14 Virus production	38
4.15 Lentiviral stock titration	38
4.16 RT-PCR	39
4.17 Western blot	39
5. ABBREVIATIONS	40
6. REFERENCES	42

RIASSUNTO

La tecnologia del DNA ricombinante è un'applicazione biotecnologica la cui importanza è di rilevanza enorme. Nel corso del presente progetto di dottorato le potenzialità dei sistemi di espressione eterologa sono state utilizzate per affrontare due diverse problematiche:

I. l'espressione ricombinante delle proteina PED e del dominio D4 di PLD1, al fine di comprendere i meccanismi alla base della loro interazione e di ricercare eventuali peptidi antagonisti

II. la generazione di linee cellulari umane stabilmente esprimenti il gene POTE2 γ e il silenziamento di altre normalmente esprimenti tale gene, al fine di valutare eventuali variazioni fenotipiche nella linea cellulare ospite.

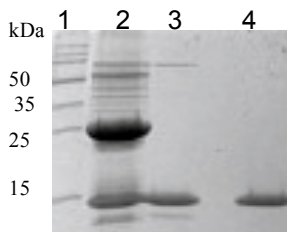
PED (Phosphoprotein Enriched in Diabetes) è una proteina citosolica di 15 kDa con differenti funzioni: è stato infatti dimostrato il suo coinvolgimento in processi proapoptotici e la sua implicazione nei processi che determinano insulino-resistenza nel diabete. Il gene *ped* è, infatti, sovraespresso nei tessuti target dell'azione insulinica (tessuto muscolare scheletrico e tessuto adiposo) dei diabetici di tipo 2. La sua sovraespressione, in cellule in coltura e in topi transgenici, induce insulino-resistenza, ma il meccanismo attraverso cui ciò avviene non è ancora ben chiaro. Attraverso diversi approcci, tuttavia, è stato verificato che PED interagisce con alcune fosfolipasi (PLD1 e PLD2) e diverse evidenze indicano l'interazione specifica con PLD1 come responsabile dell'insulino-resistenza. Il legame di PED con PLD1 non influisce sull'attività della proteina ma ne aumenta la stabilità; è stato inoltre dimostrato che l'interazione con PED è mediata dal dominio C-terminale di PLD1 (denominato D4), comprendente i residui 712-1070. E' stato infine dimostrato che bloccando l'espressione di PED (ad esempio con oligonucleotidi antisense) la resistenza all'azione insulinica è invertita e i livelli glicemici sono riportati a livelli basali. E' dunque evidente come la ricerca di eventuali molecole in grado di bloccare l'interazione PED-PLD1 rappresenti un obiettivo farmacologico di enorme interesse.

I geni POTE sono invece stati individuati attraverso tecniche bioinformatiche. In particolare, l'analisi di database di EST per geni specifici della prostata ha portato alla individuazione di una nuova famiglia di geni, denominata POTE, espressa in prostata, ovaie, testicoli e placenta ma non in tessuti normali. Sebbene la sua funzione non sia ancora nota, la presenza di dieci varianti con una identità di sequenza del 90-98% indica una alta pressione selettiva tesa al mantenimento di tale gene. Analisi mediante RT-PCR ha mostrato l'assenza di espressione di POTE in tessuti normali del seno e in normali linee cellulari epiteliali del seno, mentre esso risulta essere espresso nella maggioranza delle linee cellulari di cancro al seno, in particolare la variante 2 γ . Inoltre, normali linee cellulari epiteliali del seno trasformate dagli oncogeni ErbB-2 e Ras esprimono POTE2 γ . Tutto ciò sembra indicare il coinvolgimento di POTE2 γ nei processi di tumorigenesi del cancro al seno. Al fine di una caratterizzazione preliminare di tale gene, si è scelto sia di generare linee cellulari ricombinanti per POTE2 γ , sia di silenziare tale espressione in linee cellulari normalmente esprimenti POTE2 γ , al fine di valutare eventuali variazioni fenotipiche e, successivamente, anche genotipiche, avvenute in seguito all'espressione o al silenziamento di tale gene.

PED-D4:

Il punto di partenza è stato la messa a punto dell'espressione e purificazione della proteina PED e del dominio D4 di PLD1.

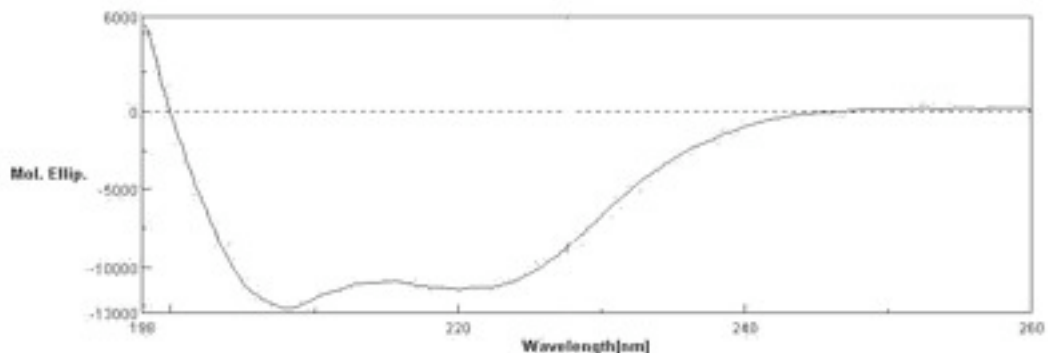
Le caratteristiche della proteina PED sono tali da avere fatto ricadere la scelta del sistema ospite per l'espressione sul batterio *E. coli*: PED è infatti solubile e di piccole dimensioni. L'amplificazione mediante PCR del c-DNA codificante per PED (messo a disposizione dal Prof. F. Beguinot, Dipartimento di Biologia e Patologia Cellulare e Molecolare, Università degli studi di Napoli Federico II) è stato il punto di partenza per il clonaggio nel vettore di espressione petM30, tramite cui PED è espressa fusa alla proteina Gst e ad un tag di poli-istidine; il ceppo ospite di *E. coli* migliore è risultato essere BL21(DE3)Star (mutante nel gene della RnaseE; ciò riduce la degradazione di mRNA) e la concentrazione ottimale di induttore (IPTG) pari a 1 mM. La resa ottenuta con queste condizioni di espressione è piuttosto elevata (circa 300 mg di proteina di fusione / l di coltura batterica) già a 37°C. L'intera proteina di fusione è stata purificata mediante FPLC su colonne His-trap (affini per l'His-tag). Per la purificazione della sola proteina PED, la proteina di fusione è stata idrolizzata in presenza della proteasi di TEV, essendo presente tra PED ed i suoi partner di fusione un linker contenente la sequenza amminoacidica specificamente riconosciuta da tale enzima. Infine, la miscela risultante dall'idrolisi è stata purificata su His-trap: essendo anche la TEV dotata di un tag di poli-istidine, PED è la sola ad essere recuperata nel flow-through. Il livello di purezza così ottenuto è $\geq 95\%$; per applicazioni in cui è stata necessaria una purezza $\geq 99\%$ è stato necessario compiere un'ulteriore purificazione prima su colonna Gst-trap (affine per la Gst) e quindi su colonna a scambio anionico MonoQ HR 5/5.



1: Protein Pefect Marker;
 2: Proteina di fusione idrolizzata in presenza di TEV proteasi (input His-trap);
 3: Eluizione dopo Gst-trap ;
 4: Eluizione dopo MonoQ HR 5/5

12%

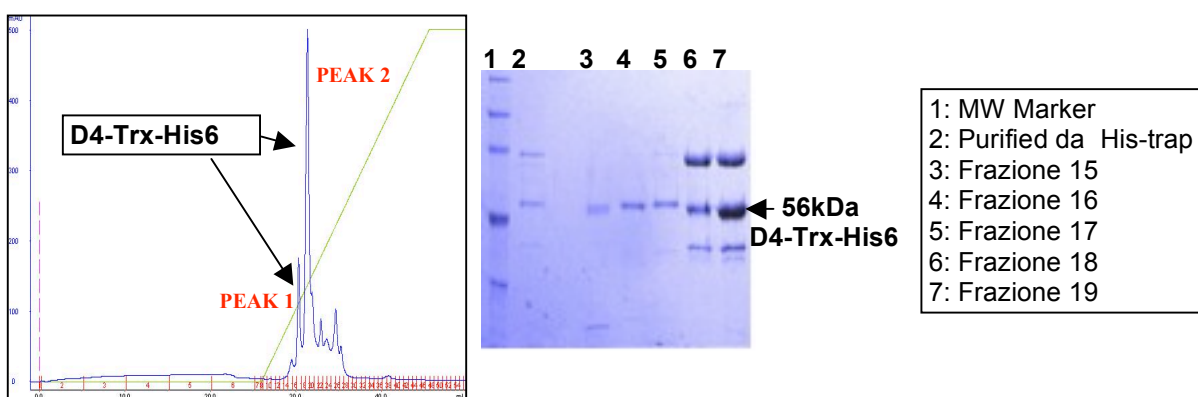
L'analisi mediante spettrometria di massa della proteina intera e digerita con tripsina ha confermato la sua identità. La caratterizzazione mediante spettroscopia CD ha invece confermato la sua corretta struttura: PED ha, infatti, all'N-terminale un dominio death effector (DED), caratterizzato dalla tipica struttura a 6 alfa-eliche, seguito da una estremità C-terminale dalla struttura irregolare. Lo spettro di dicroismo circolare registrato con la proteina pura al 99% ha evidenziato una struttura di questo tipo:



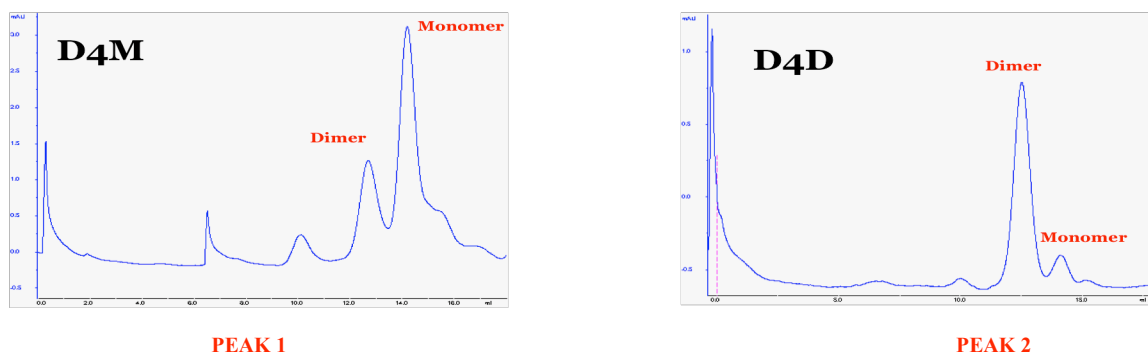
La denaturazione termica di PED, seguita mediante CD, ha mostrato un alto valore della temperatura di melting di essa (>55°C), indice di elevata stabilità della proteina; essa, inoltre, si rinatura facilmente anche dopo trattamento termico.

Anche per D4 sono stati provati diversi vettori di espressione e diversi ceppi batterici: le condizioni ottimali si sono avute col vettore pETM20 (in cui D4 è espressa fusa alla proteina TrxA e al tag di poli-istidine) in BL21(DE3)pLysS (in cui la presenza del plasmide pLysS permette un controllo più rigoroso dell'induzione dell'espressione con IPTG) in presenza di IPTG 0,1 mM, a 22°C per 16 h. Le rese di espressione, tuttavia, risultano essere abbastanza basse (circa 1 mg/l di coltura). La proteina di fusione (D4-Trx-His6) è stata quindi purificata su His-trap e poi su colonna a scambio anionico MonoQ HR 5/5; a causa dell'alto numero di cisteine presenti in D4 (5) è necessario effettuare tutte le purificazioni in presenza di TCEP 1mM. Anche in queste condizioni, comunque, D4-Trx-His6 è piuttosto instabile nel tempo. Inoltre, ogni tentativo di idrolisi in presenza della proteasi di TEV è fallito; perciò, per le analisi successive è stata utilizzata l'intera proteina di fusione D4+Trx+His6.

Inaspettatamente, la proteina di fusione dopo MonoQ HR 5/5 risulta essere presente in due picchi distinti:



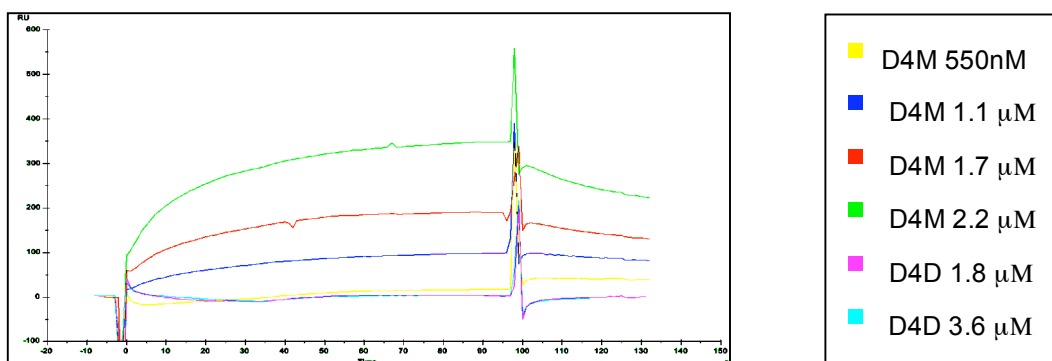
L'analisi mediante LC-MS ha confermato che entrambe le frazioni contengono la stessa proteina, che risulta essere D4+Trx+His6. Analizzando entrambe mediante gel filtration (Superdex200 HR 10/30) e su gel nativo, è risultato che nel primo picco è stata separata una forma monomerica (D4M), nel secondo una forma dimerica (D4D):



La gel filtration, ripetuta con concentrazioni differenti di NaCl nel tampone di corsa, ha mostrato che all'aumentare della concentrazione salina l'equilibrio risulta spostato verso la forma monomerica, facendo ipotizzare una interazione di tipo ionico tra le due subunità.

Esperimenti preliminari ELISA hanno confermato l'interazione di D4+Trx+His6 con PED; essa è poi stata ulteriormente validata attraverso la tecnica dell'SPR,

utilizzando un sistema Biacore 3000. PED è stato efficientemente immobilizzato sulla superficie di un sensore CM5, quindi concentrazioni crescenti di D4M e D4D sono state iniettate su esso (dopo aver verificato che Trx+His6 non lega PED): inaspettatamente, il dimero è incapace di legare PED, mentre D4 monomeric lega PED ($K_D = 2 \pm 1 \cdot 10^{-7}$)



Il saggio di legame così ottimizzato è stato utilizzato per la ricerca di peptidi inibitori dell'interazione PED-D4. A tale scopo, PED è stata idrolizzata in presenza di tripsina. La miscela di peptidi ottenuta è stata separata in differenti pool, in seguito caratterizzati mediante LC-MS; tra essi, due pool hanno dato competizione al legame di D4 con PED, uno contenente i peptidi 36-54, 36-57, 55-71, 58-71 e 72-83, ma maggiormente l'altro contenente il solo peptide 1-24, corrispondente alle prime due α -eliche del dominio DED.

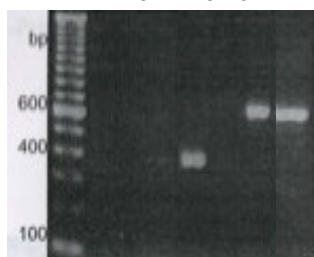
POTE2 γ :

Per la generazione delle linee cellulari esprimenti tali geni e' stato utilizzato il sistema di espressione del lentivirus, in cui lentivirus derivati da HIV-1 ma incapaci di replicarsi sono utilizzati per introdurre ed esprimere il gene di interesse in cellule di mammiferi. Una volta che il lentivirus ricombinante penetra nella cellula target, l'RNA virale e' retrotrascritto, importato attivamente nel nucleo e stabilmente integrato nel genoma dell'ospite. La selezione della linea cellulare ricombinante è infine fatta la resistenza alla Blastidina delle cellule, resistenza introdotta attraverso il lentivirus insieme al gene d'interesse.

Per esprimere il gene di interesse è stato usato il ViraPower Lentiviral Expression System (Invitrogen) per generare gli stock di virioni ricombinanti. L'amplificazione mediante PCR del gene POTE 2 γ ed il successivo clonaggio nel vettore pLenti6/V5-D-TOPO (Invitrogen) ha permesso la generazione del costrutto di espressione contenente i segnali (promotore, enhancer, gene codificante per la resistenza alla Blastidina, ecc.) necessari per l'espressione nella linea cellulare di interesse. Per la preparazione dello stock virale, i costrutti ottenuti sono stati co-transfettati (attraverso il metodo della precipitazione in BES-Calcio Fosfato) in cellule 293T (ottimali per la generazione di stock virali) insieme ad un mix di tre plasmidi che forniscono *in trans* le proteine strutturali e replicative necessarie per la produzione del lentivirus. 48 ore dopo la transfezione, il soprannatante contenente i virus e' stato raccolto, ultracentrifugato, risospeso in PBS e conservato a -80°C. Gli stock sono stati quindi titolati, ed il titolo risultante è stato $9 \cdot 10^6$ TU/ml.

I virioni così' preparati sono stati quindi utilizzati per le infezioni della linea cellulare MCF10A (cellule epiteliali di seno non cancerose), che non esprime né POTE2 γ . L'RNA totale, estratto dalle cellule ricombinanti (selezionate grazie all'acquisita resistenza alla Blastidina), è stato retro-trascritto *in vitro* in cDNA e

utilizzato come stampo per una reazione di PCR con oligo specifici per POTE2 γ (T444-T445, banda attesa di 386 bp). Lo stesso procedimento è stato effettuato con le cellule wild-type;

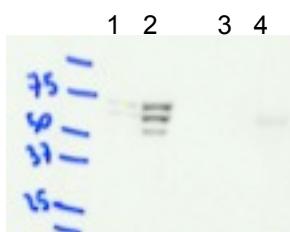


1. Marker
2. dH₂O, T444-T445 primer
3. cDNA da MCF10A wild-type, T444-T445 primer
4. cDNA da MCF10A/ POTE 2 γ T444-T445 primer
5. dH₂O, Actin primer
6. cDNA da MCF10A wild-type, Actin primer
7. cDNA da MCF10A/ POTE 2 γ Actin primer

L'analisi tramite RT-PCR, dunque, ha confermato che nelle cellule ottenute in seguito alla selezione è stato integrato il gene codificante per POTE 2 γ .

Il sistema del lentivirus è stato utilizzato anche come mezzo per silenziare POTE2 γ in una linea cellulare di cancro al seno, MCF7, che normalmente esprime tale gene. Per il silenziamento si è scelto di utilizzare il metodo dell'RNA interference (RNAi), fenomeno che permette una potente e specifica inibizione dell'espressione genica in eucarioti attraverso la degradazione di mRNA. L'espressione di short-hairpin RNA (shRNA, classe di RNA artificiali caratterizzati dall'aver una breve sequenza nucleotidica di 19-29 nucleotidi derivata dal gene da silenziare, seguita da un loop di 4-15 nucleotidi e quindi da una sequenza inversa e complementare della sequenza target iniziale) nella linea cellulare di interesse determina una degradazione dell'mRNA del gene target, causando in questo modo il silenziamento genico.

Prima di tutto, è stato ottimizzato il protocollo di silenziamento, utilizzando come target il gene *lamin*. Cellule MCF7 sono state infettate con lentivirus in grado di esprimere shRNA specifici per *lamin*; il silenziamento è stato poi verificato mediante analisi Western Blot.



- 1 MCF7 lysate, 10 μ g
- 2 MCF7 lysate, 35 μ g
- 3 MCF7-shLamin lysate, 10 μ g
- 4 MCF7-shLamin lysate, 35 μ g

Avendo quindi verificato l'effettivo funzionamento del metodo scelto, sono stati generati gli stock di lentivirus da utilizzarsi in futuro per il silenziamento del gene POTE 2 γ nelle cellule MCF7.

Gli esperimenti eseguiti nel corso del presente progetto di dottorato hanno dunque permesso di ottenere informazioni sull'interazione tra PED e D4. L'assenza di legame con D4 in forma dimerica potrebbe avere anche importanti implicazioni biologiche, poichè l'aumentata attività di PLD1 riscontrata nelle cellule sovraesprimenti PED potrebbe essere l'effetto della distorsione degli equilibri di oligomerizzazione di PLD1. È stata inoltre identificata una regione di PED di potenziale interazione con PLD1, corrispondente alle prime due α -eliche.

Le linee cellulari ricombinanti e gli stock virali esprimenti shRNA per POTE 2 γ saranno utilizzati per una caratterizzazione sia del genotipo che delle proteine espresse, al fine di rilevare eventuali variazioni.

SUMMARY

In the research project described in this thesis, all the potentialities of recombinant DNA technology have been employed to investigate two different systems, PED-PLD1 and POTE.

PED (Phosphoprotein Enriched in Diabetes) is overexpressed in skeletal muscle, adipose tissue and fibroblasts from type 2 diabetic individuals, this disease being one of the most common disorders in the world. Several lines of evidences suggest that *ped* overexpression may cause impairment of insulin-stimulated glucose transport through its interaction with PLD1 (Phospholipase D1). The mechanism by which this occurs is still unknown, but it is clear that PED lengthens PLD persistence in the cell rather than increasing its enzymatic activity.

In the present study, both PED and the D4 domain of PLD1, which is the shortest region still able to bind to PED, were expressed and purified.

Hydrolysis in the presence of TEV protease enabled the cleavage of PED from its fusion partners and its characterization. LC-MS of the entire PED protein and peptide mass fingerprinting confirmed its identity. PED α -helical structure resulted very stable, as seen by CD analysis and thermal denaturation.

Reducing conditions were used in all D4 manipulations, to avoid the formation of aggregates. Two different isoforms of D4, monomeric (D4M) and dimeric (D4D), were isolated. The nature of the intermolecular interaction in the dimeric form was checked using gel filtration chromatography at different saline concentrations.

Preliminary ELISA assays confirmed D4-PED interaction. Real-time BIA technology showed that PED only interacts with the monomeric form of D4; moreover, using trypsin-derived peptides in a competition assay, peptide 1-24 of PED resulted to be a strong competitor for D4 binding, while a mixture of peptides 36-54, 36-57, 55-71, 58-71 and 72-83 competed less efficiently.

All these findings could also have relevant biological implications, as the increased PLD1 activity promoted by PED binding *in vivo* could be the result of a shifted equilibrium of PLD isoforms.

Instead, using bioinformatics tools, the POTE gene family was identified; it consists of 11 highly homologous genes expressed in several different cancer types. In particular, POTE2 γ has aroused interest as a specific target in breast cancer therapies. Elucidation of *POTE* expression patterns, regulation and its role in cancer cells is essential to explore its therapeutic potential.

The lentivirus system was used to generate a stable POTE2 γ expressing breast cell line. This system can also be employed to express sh-RNA for gene silencing. An experimental procedure was optimized to silence the *lamin A/C* gene and recombinant lentiviruses capable of silencing *POTE* expression were generated. Further experiments are ongoing to produce anti-POTE antibodies.

1. INTRODUCTION

1.1 RECOMBINANT PROTEIN EXPRESSION

One of the most powerful applications of biotechnology is the methodology of recombinant DNA: thanks to this technology, it has been possible to develop expression systems capable of rapidly producing large quantities of proteins. This is of enormous benefit, for example, in case of proteins that can only be obtained in scarce amounts from natural compounds and/or that can't be easily purified.

Recombinant DNA technology allows the cloning of the gene of interest in an expression vector, an autonomously replicating plasmid containing all the signals necessary for the expression of the protein in a suitable host organism. The most common hosts are bacteria, since they duplicate rapidly and require easy and economic culture conditions; this allows their use to express large amounts of protein without high costs and difficulties. The most used microorganism is *Escherichia coli*: its genetics and physiology are well known and moreover it can be grown and manipulated using simple laboratory instruments. A big limit of this system, however, is the lack of enzyme systems to carry out specific post-translational modifications that many proteins need for biological activities. When such modifications are required, it is necessary to use expression systems based on eukaryotic cells (such as yeast, insect or mammalian cells). Another limit of *E. coli* is the expression of proteins as insoluble aggregates, known as inclusion bodies. In such cases, production of soluble protein can be improved by lowering the growth temperature or else recovered by renaturation from inclusion bodies; often, however, changing expression system is also the only solution.

Recombinant DNA technology has also allowed expression of the target protein fused to peptides or proteins that promote its solubilization and/or facilitates any subsequent purification. The fusion partner can then be removed if it is linked to the gene of interest by an aminoacidic sequence containing a specific protease recognition site (such as TEV protease, Thrombin, Enterokinase, etc.)¹.

Each single protein, however, is characterized by a peculiar set of properties that do not allow a standardization of expression and purification conditions that must be investigated and optimized in each case.

In the research project described in this paper, all the potentialities of recombinant expression have been employed as the starting point to investigate two different systems, PED-PLD1 and POTE.

1.2 PED-PLD1

PED (Phosphoprotein Enriched in Diabetes, Fig.1) is an ubiquitously expressed protein that controls cell proliferation and death and plays an important role in tumour development^{2, 3, 4}.

¹MAEYGTLLQDLTNNITLEDLEQLKSACKEDIPSEKSEEITTSAWFSFLE⁵⁰
⁵¹SHNKLDKDNLSYIEHIFEISRRPDLTMMVVDYRTRVLKISEEDELDTKLT¹⁰⁰
¹⁰¹RIPSAKKYKDI IROPSEEEI IKLAPPKKA¹³⁰

Figure 1: PED sequence

PED ORF is four codons different from PEA-15 (Phosphoprotein Enriched in Astrocytes): Ala→Val², Leu→Phe⁸, Tyr→Ile⁶², Ala→Gly¹²⁴⁵.

The three-dimensional structure of PED (Fig.2) consists of an N-terminal Death Effector Domain (DED) comprised of six antiparallel amphipatic α -helices closely packed around a central hydrophobic core, followed by a long and irregular C-terminal tail. The α -helices in the DED are connected by short loops and are arranged in a Greek Key topology, with $\alpha 1$ and $\alpha 2$ being centrally located. This fold represents the core structure typical of the death motif superfamily⁶

The DED domain is followed by a Protein Kinase C (PKC) phosphorylation domain (residues 99-107) and a calcium/calmodulin-dependent kinase II site (residues 110-122)⁷. PED antiapoptotic function is regulated by phosphorylation of Ser₁₁₆ and Ser₁₀₄⁸.

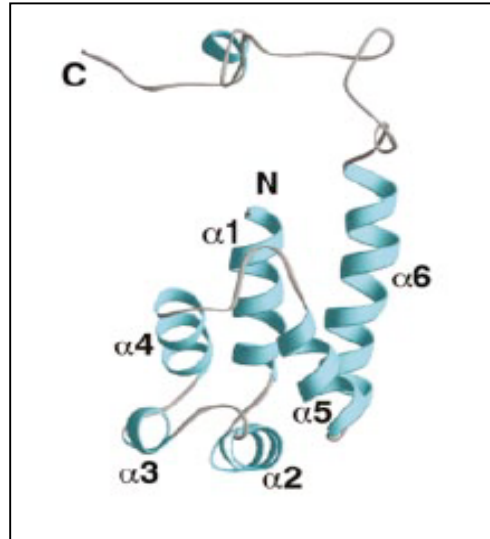


Figure 2: PED structure

Residues 2-14, 17-27, 33-37, 42-51, 61-69 and 73-89 comprise helices $\alpha 1$, $\alpha 2$, $\alpha 3$, $\alpha 4$, $\alpha 5$ and $\alpha 6$, respectively.

It has been found that PED is overexpressed in skeletal muscle, adipose tissue and fibroblasts from type 2 diabetic individuals by two to threefold. PED overexpression in normal muscle and adipose cells to levels comparable to those occurring in type 2 diabetes inhibits insulin-stimulated glucose transport and cell-surface recruitment of Glut4, the major insulin-sensitive glucose transporter⁹. Moreover, transgenic mice for PED treated with a fat diet develop diabetes. Blocking PED expression with appropriate antisense oligonucleotides in cultured cells inverts insulin resistance and brings glucose to basal levels¹⁰.

All this evidence suggests that *ped* overexpression may cause type 2 diabetes mellitus, one of the most common disorders in the world, for which it is not known whether if a single genetic defect is responsible for it or which mechanism causes impaired insulin action and secretion^{11, 12}.

Mutation experiments show that PED phosphorylation, which is responsible for PED antiapoptotic function, is not involved in these changes in glucose uptake regulatory functions¹³, so a different mechanism has to be implicated.

PED is a phospholipase D1 (PLD1) interactor which increases PLD activity. The mechanism on which this occurs is still unknown, but it is clear that PED lengthens PLD persistence in the cell rather than increasing its enzymatic activity^{10, 14}.

PLD1 is a protein widely distributed in animals, plants, fungi and bacteria and is implicated in several cellular processes that include receptor signalling, control of intracellular membrane transport and glucose transport.

The association of PLD N- and C-terminal halves constitutes its catalytic core. Individually expressed N- and C-terminal fragments of PLD1 are catalytically inactive, but, when coexpressed, PLD activity is reconstituted and direct interaction between the fragments can be observed. Interaction is observed only when N- and C-termini are coexpressed but not when they are individually expressed and mixed *in vitro*; thus, this self-association likely occurs during translation and may involve specific folding processes^{15, 16, 17}. Requirement of intramolecular dimerization to form a catalytically active enzyme introduces the possibility that intermolecular interaction may also occur. Colocalization in COS-7 cells and coimmunoprecipitation of equal amounts of differentially tagged rPLD1s implies that there is an actual dimerization between rPLD1 molecules¹⁸.

PLDs catalyse the hydrolysis of the phosphodiester bond of glycerophospholipids to generate phosphatidic acid. They are implicated in a wide range of cellular processes, most of which involve the phosphatidic acid product as an intracellular messenger¹⁵. Phosphatidic acid can also be converted to two other mediators, diacylglycerol (DAG) and lysophosphatidic acid¹⁹. DAG is a major PKC- α activator, the most common isoform of PKCs, a family of proteins that play an important role in signalling insulin activation on glucose transport²⁰.

PED induced resistance to insulin action is accompanied by an increase in DAG levels¹⁰ and activation of PKC- α ¹³, both *in vitro* and *in vivo*. This evidence suggests that, in PED overexpressing cells, PED interaction with PLD increases its activity, causing a PKC- α activation through an increase of DAG levels. PKC- α activation then downregulates insulin induction of PKC- ζ function, impairing insulin-stimulated glucose transport and Glut4 translocation (Fig.3).

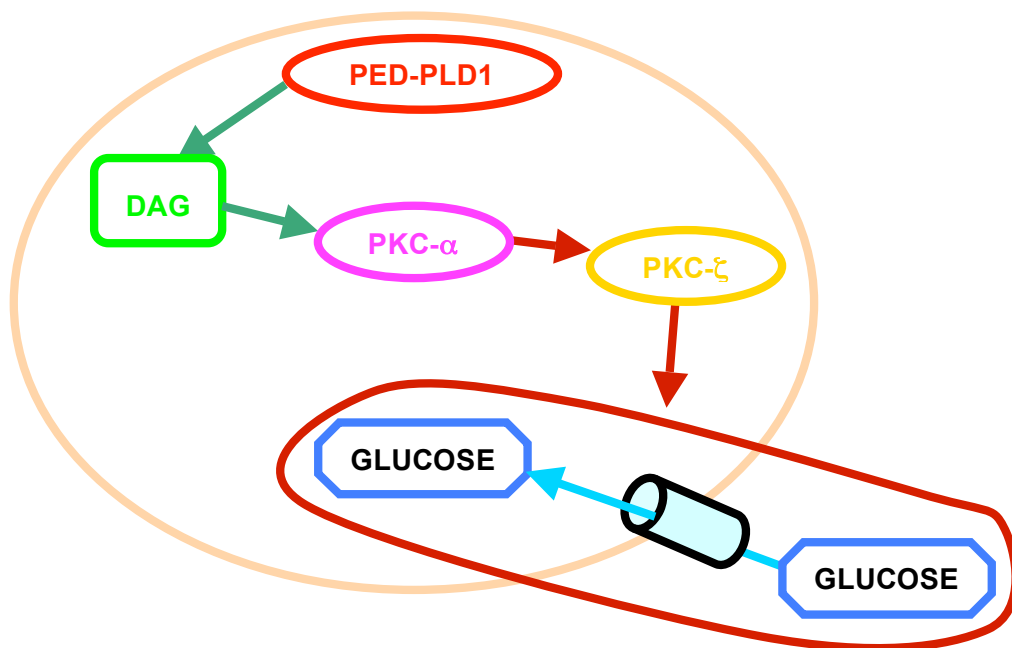


Figure 3: Effect of increased PED-PLD1 interaction

Using a two-hybrid screen, the shortest PED-interacting region of PLD1 has been identified and named D4¹⁴ (Fig.4).

712 **RSLSYPFLLPK**SQATAHELRYQVPGAVPAKV**QLLRSAADWSAGIKHHEES** 761
 762 **IHAAYIHVIENSKHYIYIENQFFISCADDKVVF**NKVGDR**IAQRILKAHRE** 811
 812 **GQRYRVYIVIPLLPGFEGDI**STGGGNAL**QAIMHFNYRTMCRGESSILEQL** 861
 862 **KPELGNKWINYISFCGLRTHAELEGN**LVTE**LIYVHSKLLIADDNTVIIGS** 911
 912 **ANINDRSM**L**GKR**DSEMAV**IVQDTETVPSVMDGKEYQAGRFARDLRLECFR** 961
 962 **LVLGYLSDPSEDLQDPVSDKFFKEI**WV**STAARNATIYDKVFRCLPNDEVH** 1011
 1012 **NLIQLRDFINKPILAKEDALRAEEELRKIRGFLVQFPLYFLSEENLLPSV** 1061
 1062 **GTKEAIVPMEVWT** 1074

Figure 4: D4 sequence

CRIII (in red), HKD domain (in pink) and CT (in green) are conserved regions critical for PLD catalytic functions²¹. D4 binds also RhoA²³; PED and RhoA interaction site overlap but are not identical²⁴.

Random mutagenesis subsequently revealed several D4 mutants unable to bind PED²³ (see Table 1).

MUTANTS NOT INTERACTING WITH PED	MUTANTS STILL INTERACTING WITH PED
I770M	H775R
H775L/E1054G	V819G
I777N	I870T
I805T	N905Y/K981N
V817E/S979R	T906S/Q1046H
N867K/D980V	N913/D1008N
W869R	G921E/K1039E
D903V/R1032P	Q975R/D999V
D904N	D999V
D904G/A912T	N1007K
A912G/L964R	V1010A
K922M/S939L	V1045A
S925R/V1001N	
M941T	
A948V/V1045M	
E958P	
D976V	
D1008Y	

Table 1

The mutations are spread through out D4 and are not localized to any particular PED binding site; all attempts to identify this site have been unsuccessful^{14, 24}.

Because multiple overlapping PED clones were identified in the two-hybrid screen, PED region 53-112 was assumed to be the PLD1 interacting site. Phosphorylation of Ser₁₀₄ doesn't affect PED-PLD1 interaction.

1.3 REAL-TIME BIA

Real-time BIA (Biomolecular Interaction Analysis) is a technology that allows the monitoring of biomolecular interactions in real time without labelling any of the

components. An advantage of this system is that high purity or large amounts of the biomolecules are not strictly required^{25, 26, 27}. It combines the use of biosensors with Surface Plasmon Resonance (SPR).

SPR is an optical phenomenon arising in thin metal under conditions of total reflection that produces a sharp dip in the intensity of reflected light at a specific angle (the resonance angle). The position of this angle depends on several factors, including the refractive index of the medium close to the non-illuminated side of the metal film. Refractive index is directly correlated to the concentration of dissolved material in the medium. By keeping other factors constant, SPR can be used to measure changes in the concentration of molecules in a surface layer of solution in contact with the sensor surface. In Real-time BIA, one of the component (named ligand) is covalently attached to a dextran coated gold surface²⁸. A solution of the other component (named analyte) is then injected over the surface at continuous flow. As molecules from solution bind to the ligand, the resonance angle changes and a response is registered (Fig.5).

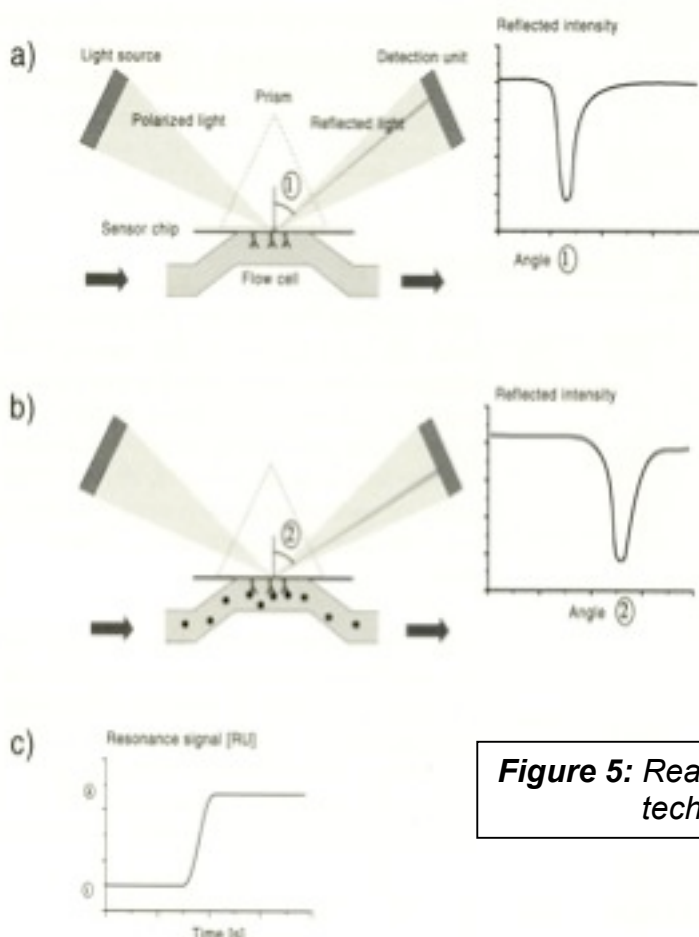


Figure 5: Real-time BIA technology

In a typical experiment, the analyte is injected over the sensor surface with the immobilized ligand, and a full record (named sensorgram) of the progress of the biospecific interaction can be obtained by continuously measuring the SPR angle versus time. After the association phase, buffer washes out the analyte and the loss of bound analyte from the sensor is also registered (Fig.6).

Data from the sensorgram can also be used to calculate kinetic and thus equilibrium constants²⁵.

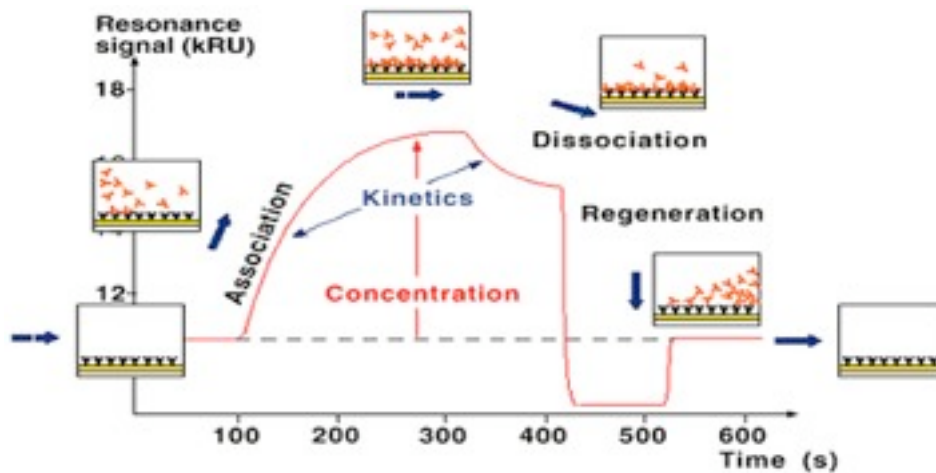


Figure 6: A typical sensorgram

1.4 POTE

Since the publication of the human genome sequence, a new era for cancer research has been opened²⁹. Search for Expressed Sequence Tag (EST) in the human genome sequence has been made possible with the help of bioinformatics. The development of a computer-based screening strategy has allowed the identification of several genes that are expressed in prostate cancer³⁰. Using this approach, a new gene family has been discovered, *POTE*, which is selectively expressed in normal prostate, testis, ovary and placenta, as well as in prostate cancer³¹. The *POTE* family consists of at least 11 genes located on chromosomes 2, 8, 14, 15, 18, 21 and 22. Although *POTE* function is unknown, the presence of so many variants with 90-98% sequence identity indicates selective pressure to maintain the gene. *POTE* family genes (Fig.7) appear to be primate-specific; they encode for a highly homologous group of proteins that contains five to seven ankyrin repeats and a spectrin domain at its C-terminus, suggesting interaction with the cytoskeleton. Preliminary studies have localized *POTE* to the plasma membrane³².

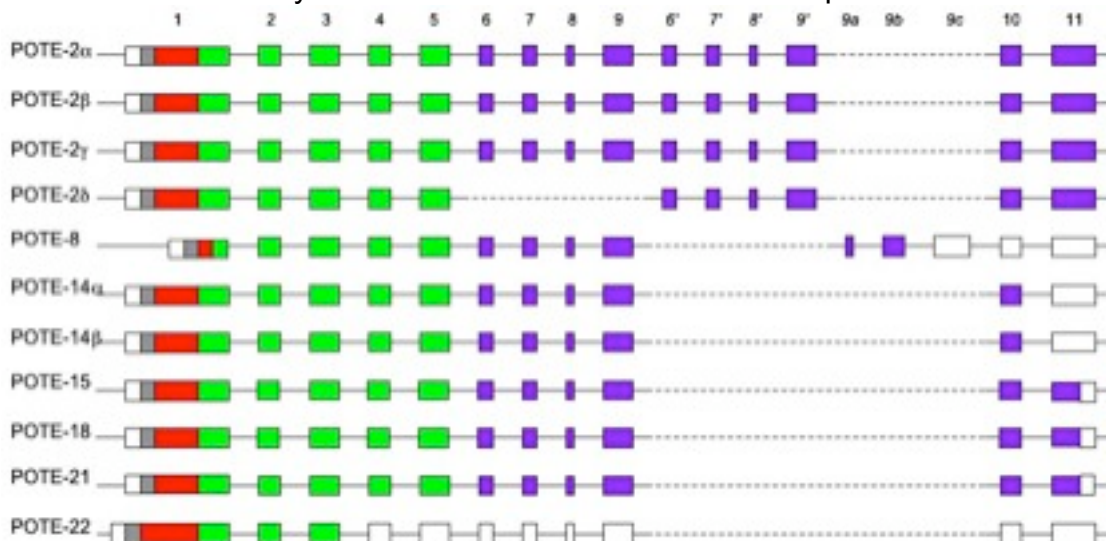


Figure 7: POTE variants in the genome
Exons are represented as square boxes. Red boxes denote N-terminal repeats, green boxes ankyrin repeats, blue boxes helical C-terminus²⁸.

Recent studies shows that POTE is also expressed in several other different cancer types. In particular, POTE expression in breast cancer has been investigated³³. PCR on cDNAs from breast tissues³¹ and RT-PCR of RNA from the MCF-10A breast cancer cell line³³ showed that POTE transcripts are not present in these samples. Instead, four out of five breast cancer cell lines express POTE, and the variants found in cancer cells are mostly POTE-2 α and POTE-2 γ (Fig.8).



Figure 8: POTE expression
 1, no DNA; 2, MCF10A cDNA; 3, MCF-7 cDNA; 4, HTB-30 cDNA;
 5, MDA-MB-231 cDNA; 6, HTB-19 cDNA; 7, HTB-20 cDNA; 8, ZR-75-1 cDNA

Moreover, MCF-10A cells transformed by the oncogenes ErbB-2 and Ras also express POTE, suggesting that it is an event that occurs during tumorigenesis³³.

All these findings suggest that *POTE* may be activated during tumorigenesis in many but not all breast cancers, implying that POTE could be used as a specific target for breast cancer therapies.

1.5 LENTIVIRAL EXPRESSION SYSTEM

The lentiviral expression system uses lentivirus to deliver a target gene to mammalian cells. A lentivirus is a replication-incompetent, HIV-1 based lentivirus that can be used in a wide range of both dividing and non-dividing cells, broadening its potential application beyond those of other virus-based retroviral systems. It can be used also for *in vivo* delivery of the target gene and the presence of multiple features designed to enhance the biosafety of the system eases its manipulation³⁴.

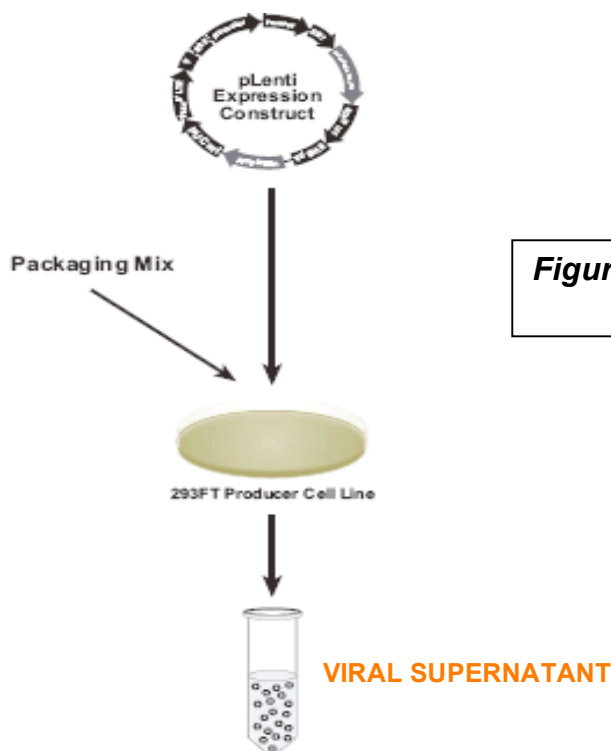


Figure 9: Production of recombinant lentivirus

To generate a recombinant lentiviral stock, the target gene is cloned into an expression vector containing all the signals for its expression in mammalian cells as well as elements that allow packaging of the construct into virions. The vector and a mixture of plasmids, supplying the helper functions as well as structural and replication proteins *in trans* required to produce the lentivirus, are then cotransfected in HEK293T producer cells. The recombinant lentivirus can be harvested in the supernatant after 48 hours, titered and transduced into the mammalian cell line of interest (Fig.9).

Once the lentivirus enters the target cell, viral RNA is reverse-transcribed, actively imported to the nucleus and stably integrated in the genome. Once integrated, the lentiviral genome is no longer capable of producing packageable viral genome³⁵. A stable transduced cell line can be selected using the Blasticidin resistance that is introduced with the target gene.

1.6 AIM OF THESIS

In the study illustrated in this paper, DNA recombinant technology has been employed as the starting point for elucidating PED-PLD1 interaction and for both expressing and silencing *POTE* in suitable cell lines.

To date, very little is known about the PED-PLD1 interaction, which is in some way involved in the pathogenesis of type-2 diabetes mellitus. In the present work, PED and the D4 domain of PLD1 have been expressed and characterized. Real-time BIA has been used to set up an *in vitro* binding assay, to obtain new elucidations on their interaction. Moreover, this assay has been used to screen PED-derived antagonists peptides in a competition assay. This experiment had served not only to further characterize PED-PLD1 interaction, but also to look for antagonists which could be used as pharmacological molecules in the therapy of type 2 diabetes.

Instead, understanding *POTE* expression patterns, regulation and its role in cancer cells is essential to explore its therapeutic potential. For this reason, a recombinant *POTE* expressing breast cancer cell line has been created, using the lentiviral expression system. This system has also been employed to generate recombinant virus capable of silencing *POTE* expression in breast cancer cell lines.

2. RESULTS

2.1 PED-D4 INTERACTION

2.1.1 PED cloning, expression and purification

PED ORF (kindly provided by Prof. F. Beguinot, Dipartimento di Biologia e Patologia Cellulare e Molecolare, Università Federico II di Napoli) was amplified by PCR using two primers allowing its cloning in 5 different *E. coli* pETM expression vectors³⁶ (Table 2).

EXPRESSION VECTOR	N-TERMINAL TAG	SELECTABLE MARKER
pETM-11	6-His	Kan
pETM-20	6-His+ TrxA	Amp
pETM-30	6-His+ Gst	Kan
pETM-52	6-His+ DsbA	Kan
pETM-60	6-His+ NusA	Kan

Table 2

Expression of all recombinant proteins is under the control of the T7 promoter in these vectors, which contain a TEV recognition site between the protein of interest and its fusion partners. Expression levels in the *E. coli* strain BI21(DE3) (1mM IPTG, 3 h @ 37°C), were evaluated through SDS-PAGE analysis of total, soluble and micropurified fractions of 1.5 ml of cell cultures. Best results were obtained using the recombinant pETM30 (Fig.10).

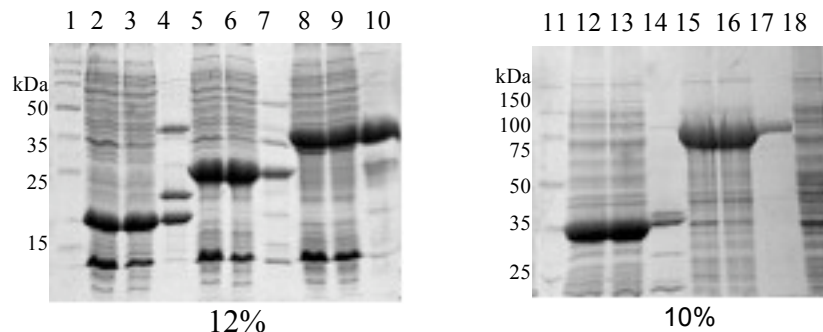


Figure 10: SDS-PAGE analysis of the expression levels

1, 11: Perfect Protein Marker; 2, 3, 4: pETM11, total, soluble and micropurified fractions (expected protein size: 16.8 kDa); 5, 6, 7: pETM20, total, soluble e micropurified fractions (expected protein size: 28.6 kDa); 8, 9, 10: pETM30, total, soluble e micropurified fractions (expected protein size: 41.6 kDa); 12, 13, 14: pETM52, total, soluble e micropurified fractions (expected protein size: 37.7 kDa); 15, 16, 17: pETM60, total, soluble e micropurified fractions (expected protein size: 70.8 kDa); 18: wild-type, soluble fraction

Further experiments showed that using the strain BI21(DE3)star it was possible to obtain up to 300 mg of PED fused to Gst+His6/ litre of bacterial culture.

PED+Gst+His6 was purified on a His-trap column and, after dialysis, hydrolyzed in the presence of TEV protease. To recover PED alone, the reaction mixture was again loaded on a His-trap column: in this case, PED is recovered in the flow-through, while fusion partners, undigested protein and TEV protease (that also

has an His-tag at its N-terminus) bind to the column. At this point, PED is about 95% pure.

To obtain greater than 99% purity, PED obtained from the previous step was then loaded on a Gst-trap column and the flow-through, after dialysis, eventually purified on an anionic exchange column MonoQ HR 5/5 (Fig. 11):

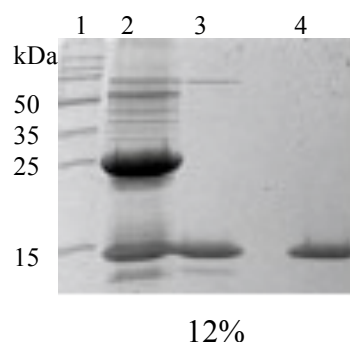


Figure 11: PED purification
1: Perfect Protein Marker; 2: PED+Gst+His6 after hydrolysis in presence of TEV protease; 3: Elution after Gst-trap; 4: Elution after MonoQ HR 5/5 purification

2.1.2 PED characterization

2.1.2a Mass spectrometry

PED molecular weight was determined by LC-MS. 0.5 μ g were loaded on a BioBasic Column C18 50x2 mm ID and then analyzed by Mass Spectrometry (Fig. 12). The resulting value is 128 amu higher than the theoretical one: this is due to an additional glycine-alanine sequence introduced at the N-terminus during the cloning.

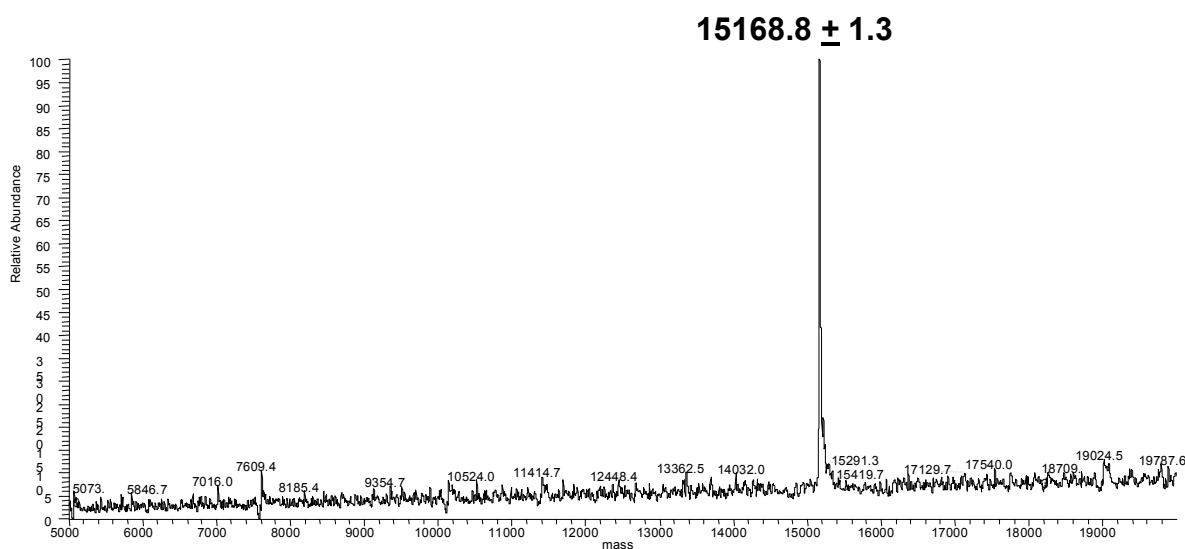


Figure 12: Mass spectrum of recombinant PED

LC-MS of the trypsin-treated protein also confirmed PED identity (Fig. 13).

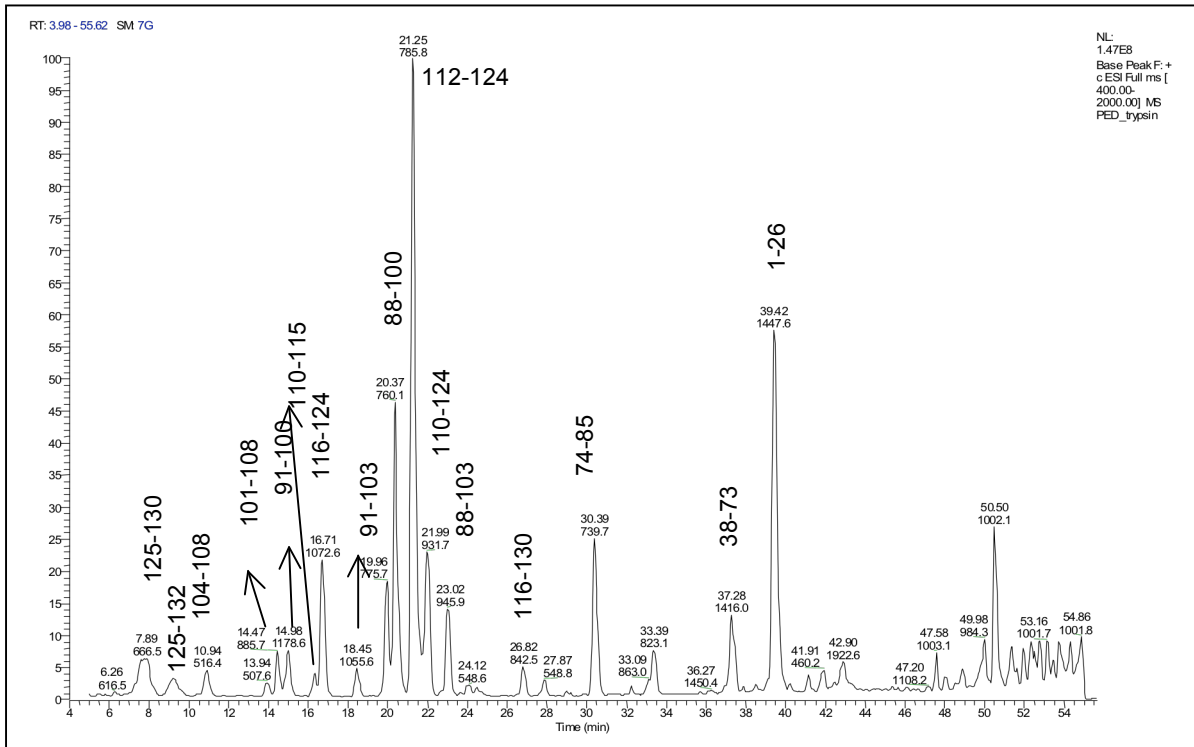


Figure 13: Mass spectrum of trypsin-treated recombinant PED

2.1.2b 3-dimensional structure

Previous NMR experiment had shown that PED has a death-effector domain at its N-terminus, characterized by a typical structure of 6 α -helices, while the C-terminus is unstructured⁶.

To assess the recombinant protein folding, a CD analysis of recombinant PED was performed. The result was a spectrum typical of α -helical structures, with a first minimum at 208 nm and a second one at 221 nm. This confirms that the protein is correctly folded (Fig.14).

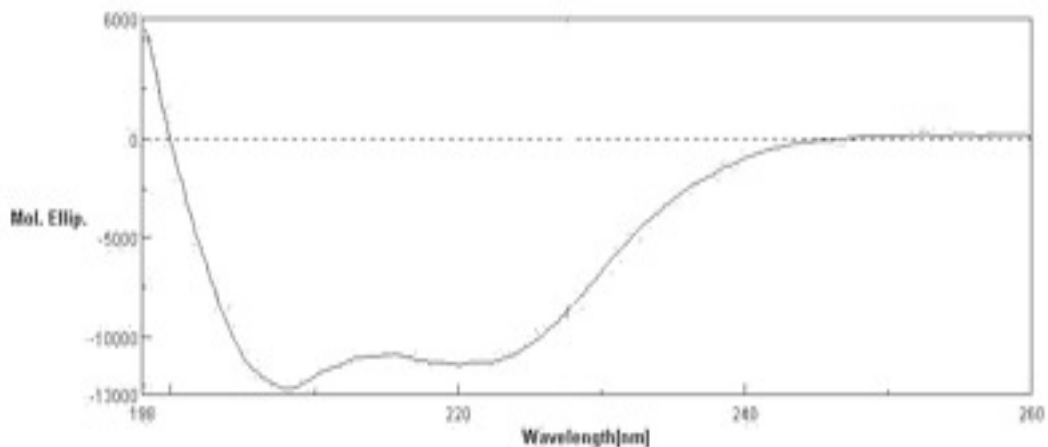


Figure 14: CD spectrum of recombinant PED
PED concentration is $1.7 \cdot 10^{-5} M$ in Tris-HCl 50 mM, pH 7.5.
Temperature is set at 10°C

PED stability was also assessed using CD spectroscopy. Thermal denaturation of PED was performed, arising the temperature from 10 to 70 °C and changes in its response at 222 nm were registered. The result was that PED denaturation occurs at a temperature higher than 55°C (Fig.15), asserting that PED has a very stable and compact structure.

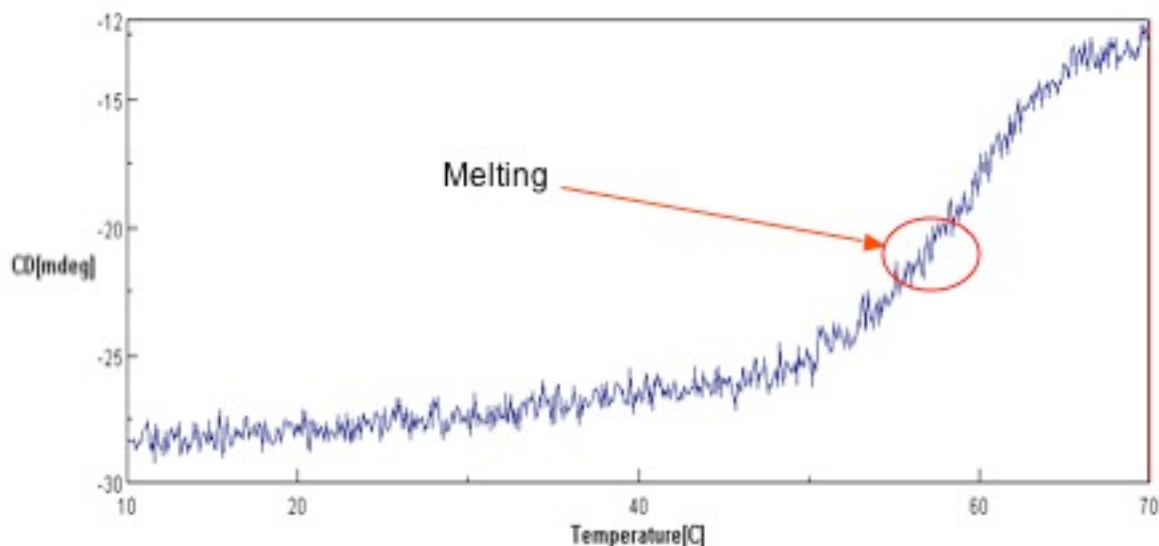


Figure 15: Thermal denaturation of PED, as monitored by CD
 PED concentration is $1.7 \cdot 10^{-5} M$ in Tris-HCl 50 mM, pH 7.5. Temperature is scanned from 10 to 70°C at $\lambda=222nm$

Moreover, PED is promptly refolded after thermal denaturation, as shown comparing the CD spectrums of the protein at 10°C, 70°C and then 20°C after thermal denaturation (Fig.16). At 70°C, in fact, the protein is totally unfolded, while at 20°C most of the α -helical structure is recovered.

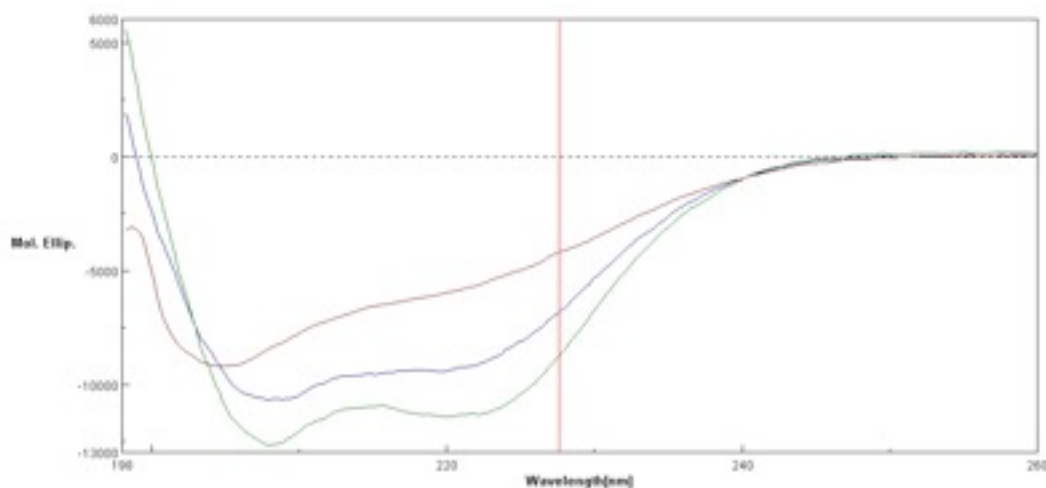


Figure 16: PED refolding after thermal denaturation
 PED concentration is $1.7 \cdot 10^{-5} M$ in Tris-HCl 50 mM, pH 7.5. The starting temperature is 10°C (green curve), it is raised to 70°C (brown curve), then lowered to 20°C (blue curve)

The state of PED oligomerization was determined by gel filtration. 100 μ g of PED were loaded on a Superdex75 10/300 GL column, previously calibrated, in Sodium phosphate buffer 20mM, NaCl 150 mM, pH 7.5. PED elution volume (11.02 ml) was the same of a protein with a molecular weight of about 35 kDa, showing its dimeric nature. Interaction is not due to the formation of disulfide bridges, since no difference was observed by loading PED on a SDS-PAGE with and without reducing agents.

Several attempts to crystallize PED have so far failed; this is probably due to the high chain flexibility of the C-terminal end of the protein, that doesn't allow the formation of crystallization nuclei.

2.1.3 D4 cloning, expression and purification

The D4 domain of hPLD1 was also amplified from a cloning vector kindly provided by Prof. F. Beguinot, Dipartimento di Biologia e Patologia Cellulare e Molecolare, Università Federico II di Napoli. The expression results with all five vectors (see Table 1) were poor but the vector pETM20 in BI21(DE3)pLysS *E.coli* (0,1mM IPTG, 16h @ 22°C) yielded sufficient protein (1mg/litre of culture) for our purposes.

Due to the high number of cysteines (5), to suppress the formation of disulfide-linked aggregates and to obtain reproducible results all purifications had to be performed in the presence of TCEP (1mM) containing buffers. However, also in these conditions the protein is quite unstable, showing a strong tendency to be degraded. Furthermore, any attempt to cleave D4 from its fusion partners failed, so the whole protein (named D4+TrxA+His6) was used for all subsequent experiments.

The fusion protein was purified on His-trap columns, followed by anion exchange chromatography on a MonoQ HR 5/5 column. Surprisingly, D4+TrxA+His6 was eluted at both 220 and 280 mM NaCl (Fig. 17)

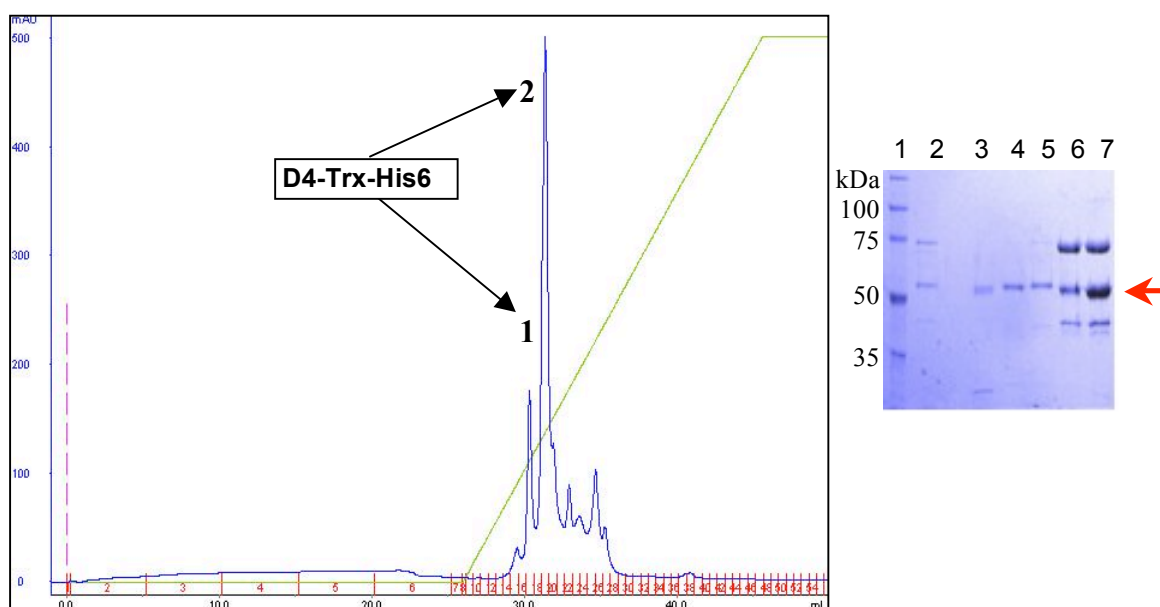


Figure 17: D4+Trx+His6 anionic exchange chromatography
 10% SDS-PAGE- 1, Perfect protein marker; 2, Input; 3, Fraction 16; 4, Fraction 17; 5, Fraction 18; 6, Fraction 19; 7, Fraction 20. The red arrow indicates D4+Trx-His6

Other proteins in fractions 18-19 were separated from D4+Trx+His6 by a Superdex200 HT 10/30 gel filtration (Fig.18).

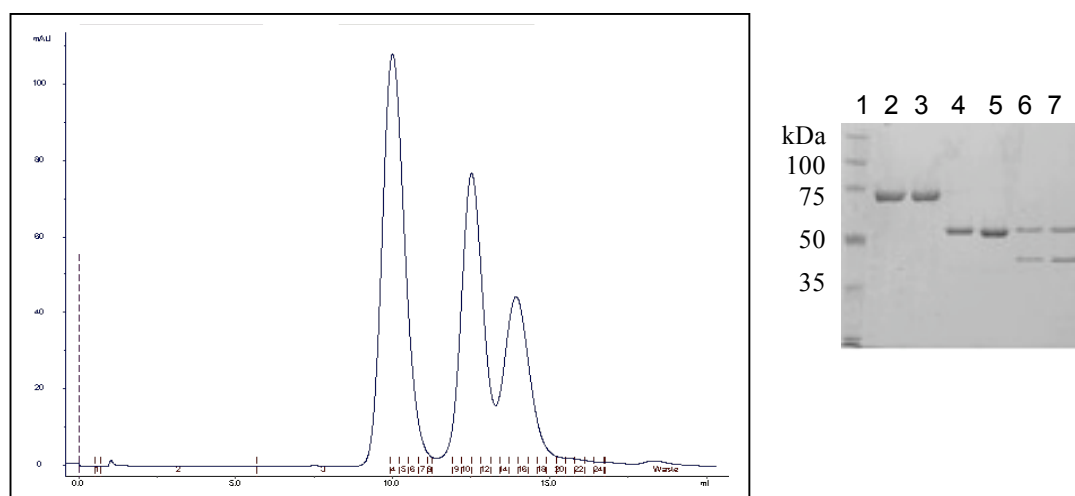


Figure 18: Gel filtration analysis of peak 2 eluted from MonoQ HR 5/5 10 % SDS-PAGE- 1, Perfect protein marker; 2,3 Fractions 4 and 5; 4,5 Fractions 10 and 11; 6, 7 Fractions 14 and 15

All proteins were subsequently analyzed by LC-MS. 0,5 µg from each fraction were loaded on a Jupiter Column C4 250x2 mm ID for LC-MS analysis. Both proteins corresponding to peak 1 of MonoQ HR 5/5 (named D4M) and fractions 10-11 of Superdex 200 (named D4D) have a mass corresponding to that expected for D4+Trx+His6 (Fig.19). The remaining proteins resulted to be bacterial proteins unrelated to D4, as determined by peptide mass fingerprint analysis of peptide obtained by trypsin digestion.

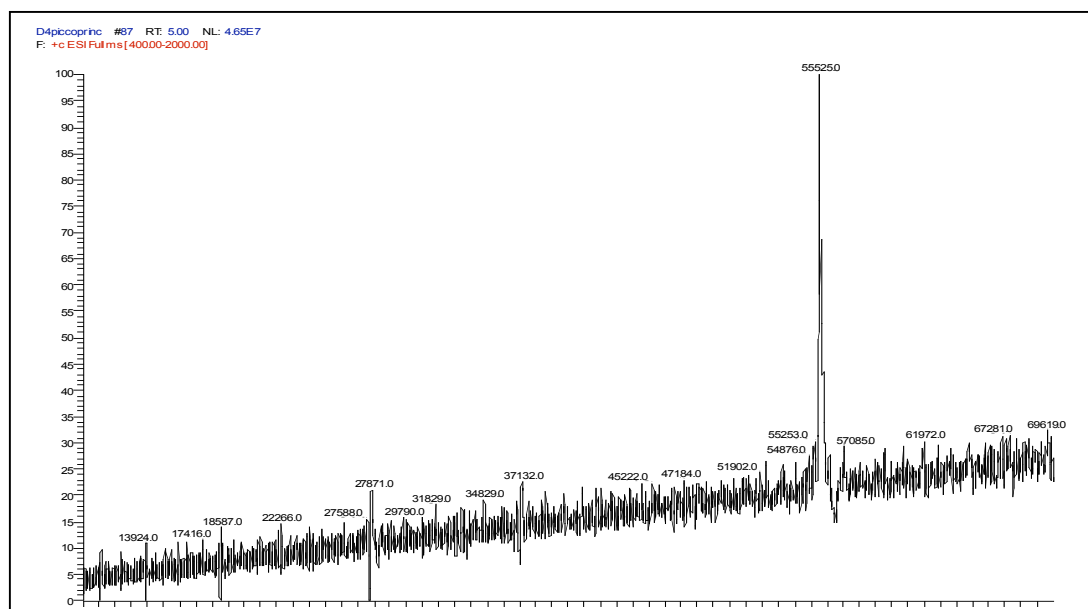
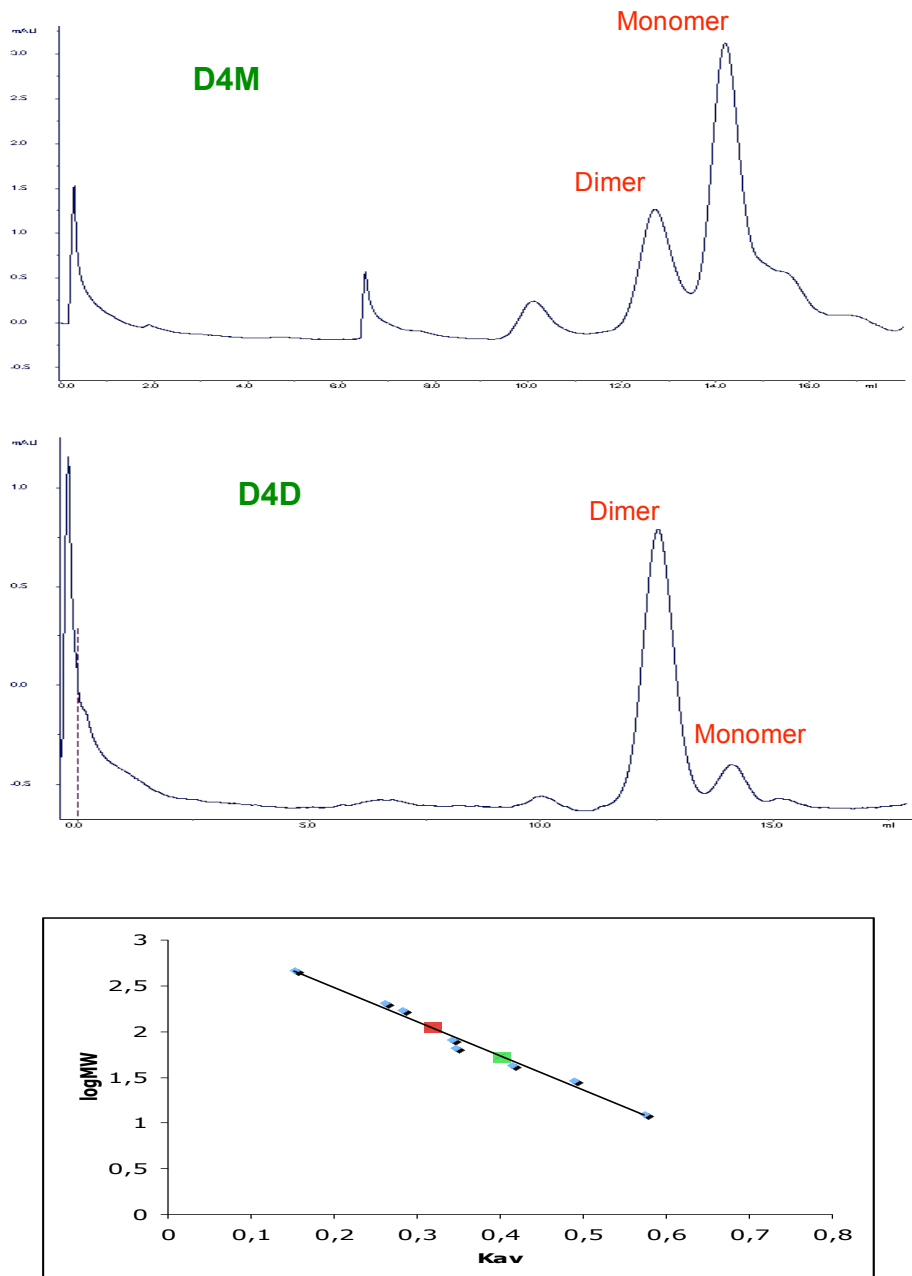


Figure 19: Mass spectrum of D4M and D4D
The resulting mass from MS analysis is about 131 amu lower than the theoretical one (55657,4 amu): this is due to the loss of the first Methionine during expression, an event that often occurs.

2.1.4 D4 dimerization

D4M and D4D were analyzed by gel filtration on a Superdex200 HR 10/30 HR 10/30 column, previously calibrated. The results showed that D4M corresponds to a monomeric form, while D4D is mainly dimeric (Fig.20).



	Main peak Ve (ml)	Resulting MW (kDa)
D4M	13,698	112
D4D	12,424	54

Figure 20: Gel filtration analysis of D4M and D4D.

This result was also confirmed by loading D4M and D4D on a 10% native gel.

The monomeric-dimeric equilibrium was shown to be sensitive to changes in the ionic strength of the buffer. Particularly, at high saline concentration the monomeric form is preponderant (Fig.22).

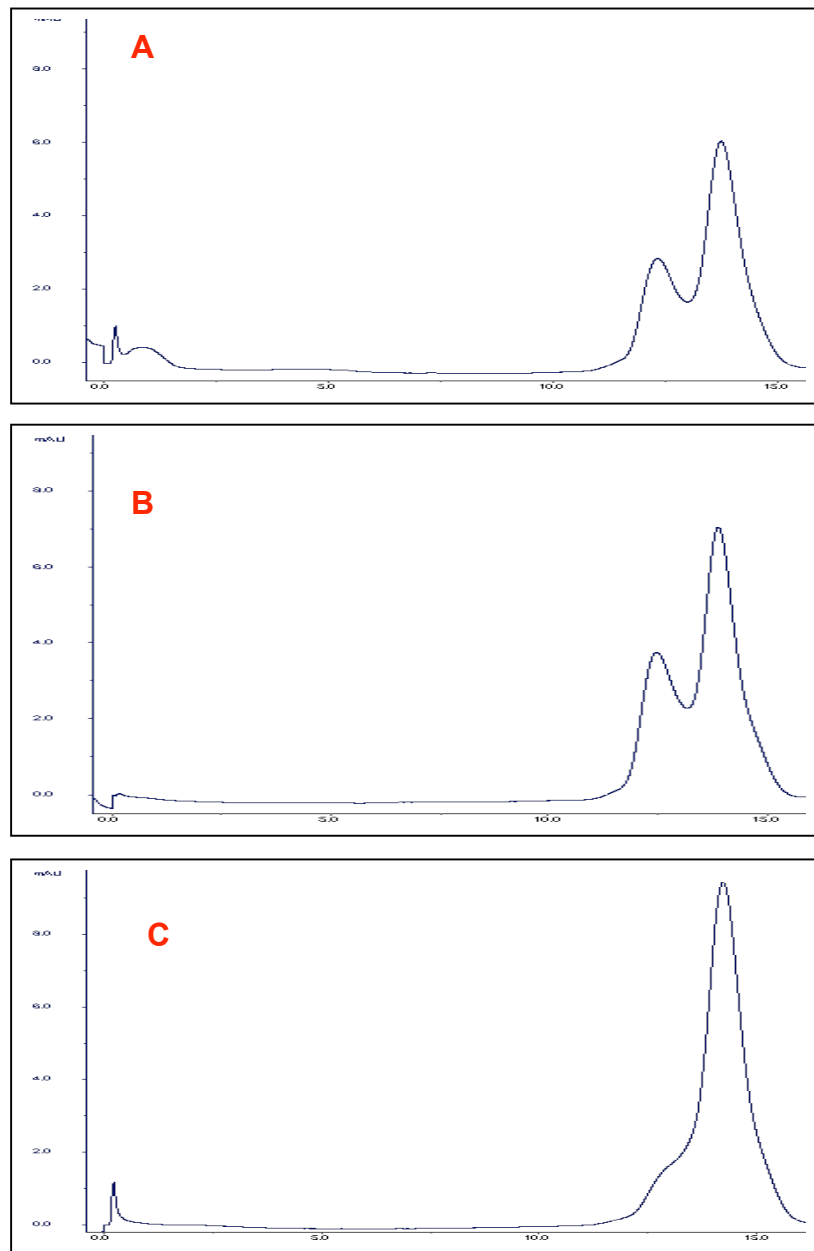


Figure 22: Effect of ionic strength on D4+Trx+His6 dimerization
A: Buffer Sodium phosphate 20 mM, NaCl 50 mM, pH7,5; B: Buffer Sodium phosphate 20 mM, NaCl 250 mM, pH7,5; C: Buffer Sodium phosphate 20 mM, NaCl 1 M, pH7,5

2.1.5 PED-D4 binding

2.1.5a ELISA assays

An ELISA assay was set up to check the binding of D4+Trx+His6 to recombinant PED. Preliminarily, anti-PED rabbit serum was dosed against PED (Fig.23).

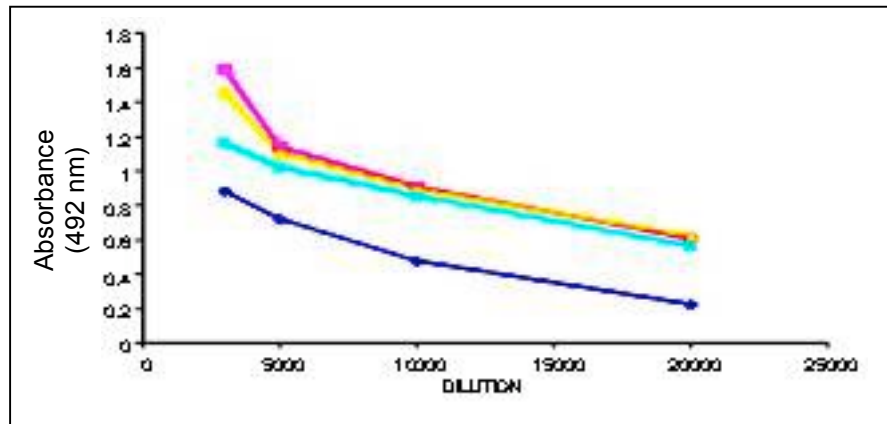


Figure 23: Anti-PED serum dosage

- PED 0,2 µg/ml
- PED 2 µg/ml
- PED 10 µg/ml
- PED 20 µg/ml

The assay was performed coating the wells with different concentrations of pools of D4M and D4D; then, increasing amounts of PED were added. Detection was achieved using 1:10000 dilution of anti-PED serum. The assays confirmed the binding of PED to D4+Trx+His6 (Fig.24)

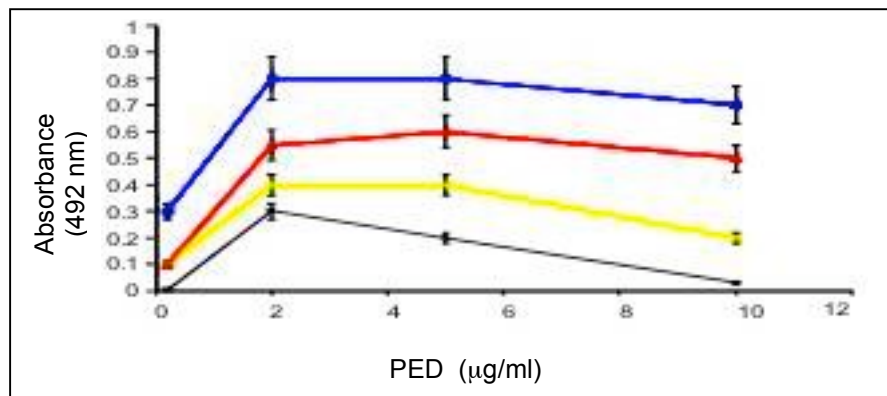


Figure 24: ELISA binding assay

- D4+Trx+His6 0,2 µg/ml
- D4+Trx+His6 2 µg/ml
- D4+Trx+His6 10 µg/ml
- D4+Trx+His6 40 µg/ml

2.1.5b: Surface Plasmon Resonance

The interaction between PED and D4+Trx+His6 was further assessed by SPR using a BIACORE 3000 system. PED was efficiently immobilized on the sensor surface, obtaining a signal of about 4000 RU. Solutions of Trx+His6 concentrated up to 3,6 µM were first injected at a 30 µl/min flow rate, using HBS buffer, pH 7.4, and no interaction was detected. Then increasing concentrations of D4+Trx+His6 from different fractions were analyzed. The results were different depending on whether D4M and D4D were used: using the dimeric protein, D4D, no binding to immobilized

PED was to detected, while using fractions containing the monomeric D4M, dose-dependent binding curves were readily observed (Fig.25).

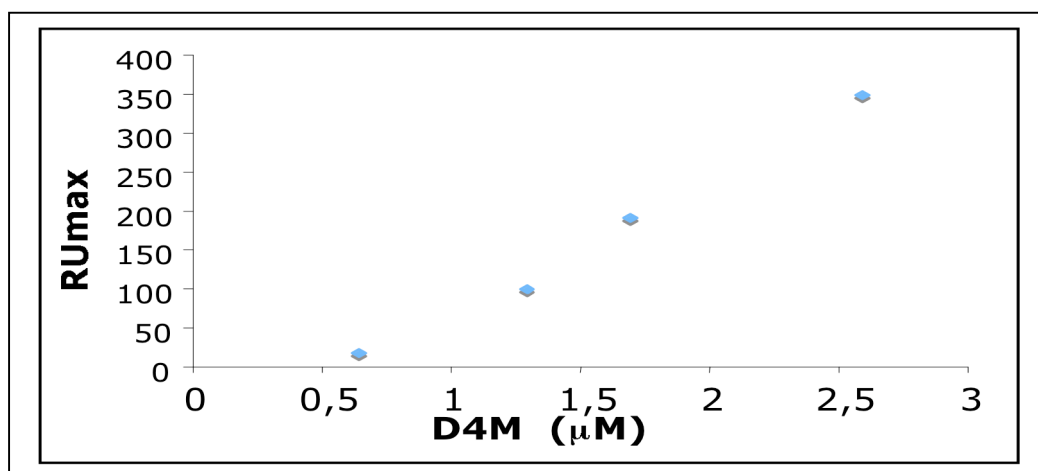
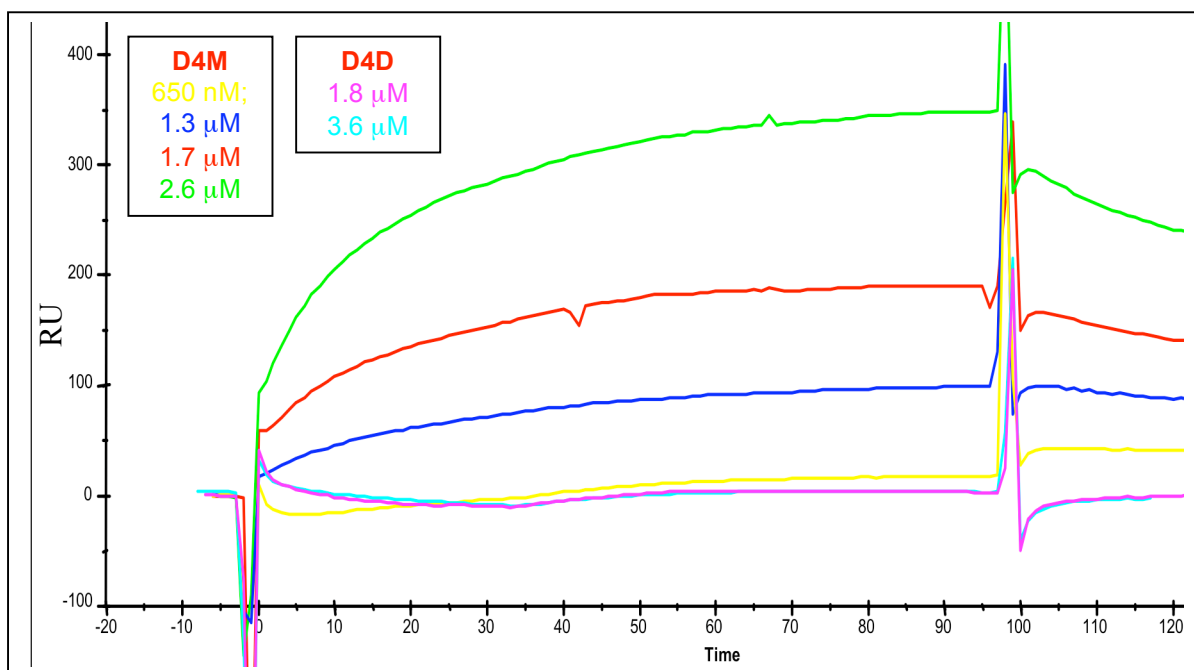


Figure 25: SPR binding assay

D4M (monomeric) binds to PED and has a dissociation constant of $2 \pm 1 \cdot 10^{-7}$ M (as calculated with the BIAevaluation software).

2.1.6 Competition assay

The Biacore 3000 system was also used to set up a competition assay to identify PED peptides able to compete with D4-PED binding.

To this aim, PED was hydrolyzed in the presence of trypsin; the reaction was stopped by adding PMSF 0,5 mM; LC-MS analysis of the protein confirmed digestion. Solutions of D4M were then mixed with solutions of undigested and trypsin-treated PED, and injected on the PED-coated chip (Fig.26).

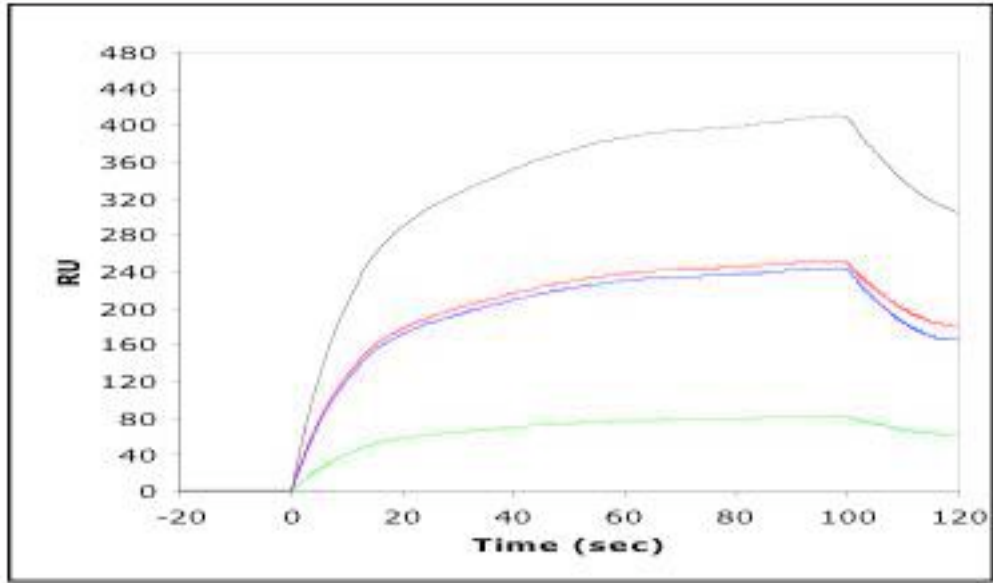


Figure 26: Sensorgrams of PE-D4 competition.
 --- D4M 2µM
 --- D4M 2µM + PED 8 µM
 --- D4M 2µM + trypsin-treated PED 8 µM
 --- D4M 2µM + trypsin-treated PED 20 µM

The result was an 80% signal reduction when D4M was mixed with PED in a 1:4 ratio, while a 1:4 ratio D4M: trypsin-treated PED reduced the signal by 41%, and the result was almost the same with a 1:10 ratio (Fig.27).

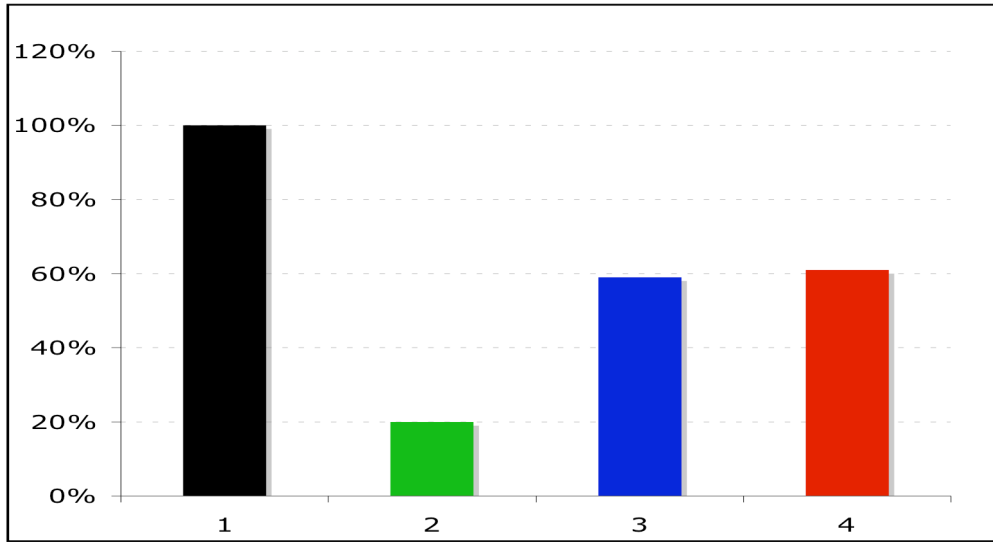


Figure 27: Sensorgrams of PED competition.
 1 D4M 2µM
 2 D4M 2µM + PED 8 µM
 3 D4M 2µM + trypsin-treated PED 8 µM
 4 D4M 2µM + trypsin-treated PED 20 µM

110 μg (7.2 nmol) of PED were then hydrolyzed in presence of trypsin and loaded on a HPLC C18 column for separation. 9 pools of peptides were collected (Fig.28).

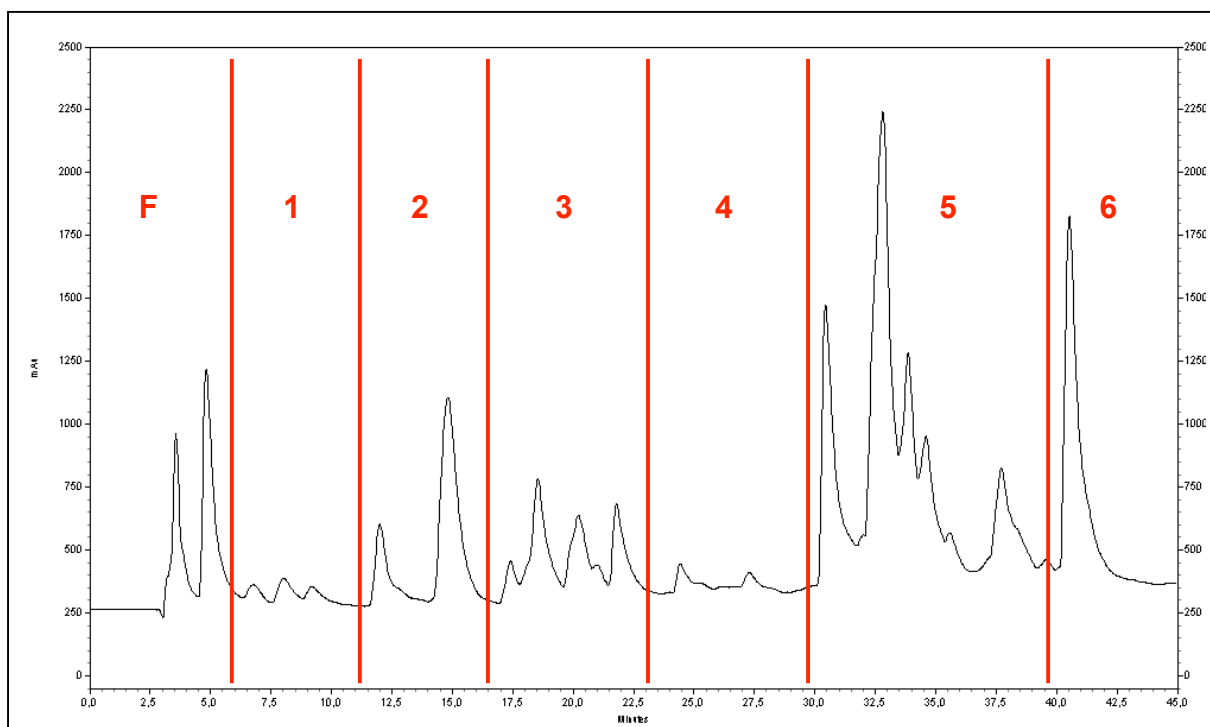


Figure 28: HPLC of trypsin-treated PED

Each pool was then lyophilized, resuspended in 100 μl of H_2O and characterized by LC-MS (Table 3).

POOLS	PED PEPTIDES IDENTIFIED BY LC-MS
F	---
1	---
2	²⁹ EDIPSEK ³⁵ , ¹⁰⁸ YKDIIR ¹¹³ , ¹²³ LAPPPKKA ¹³⁰ ;
3	⁸⁹ ISEEDELDTK ⁹⁸ , ¹¹⁰ DIIR ¹¹³ , ¹¹⁴ QPSEEEIIK ¹²²
4	---
5	³⁶ SEEITTGSAWFSFLESHNK ⁵⁴ ; ³⁶ SEEITTGSAWFSFLESHNKLDK ⁵⁷ ; ⁵⁵ LDKDNLSYIEHIFEISR ⁷¹ ; ⁵⁸ DNLSYIEHIFEISR ⁷¹ ; ⁷² RPDLLTMVVDYR ⁸³
6	⁻² GAMAEYGTLQDLTNNITLEDLEQLK ²⁴

Table 3

PED numbering starts at -2 because of the GA dipeptide introduced during the cloning upstream ¹Met.

Assuming a total recovery of the protein, concentration of each peptides was supposed 72 μM . 20 μl of pools 2, 3, 5 and 6 were used for the competition assay with D4M 1 μM , in a final volume of 90 μl (Fig.29).

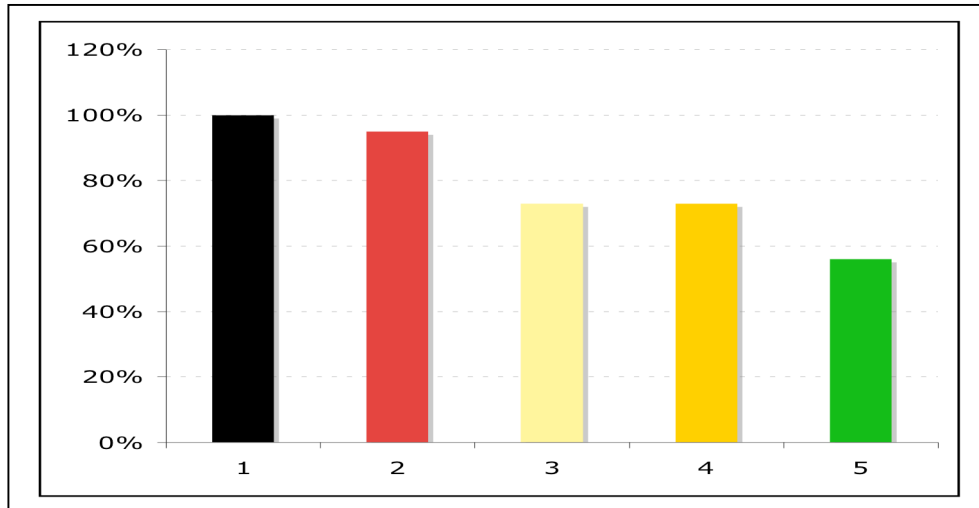


Figure 29: Competition assay

- 1 D4M 1 μ M
- 2 D4M 1 μ M + 20 μ l pool 2
- 3 D4M 1 μ M + 20 μ l pool 3
- 4 D4M 1 μ M + 20 μ l pool 5
- 5 D4M 1 μ M + 20 μ l pool 6

Pool 3 and 5 gave a reduced signal, but pool 6, corresponding to peptide $^{-2}\text{G-K}^{24}$ alone, reduced this signal further to 50% of its original value.

2.2 POTE2 γ

2.2.1 Lentivirus production

The lentiviral expression system has been used to deliver the gene in the cell line of interest. The protocol to produce the lentiviral stock has been optimized to obtain the highest viral titre.

Initially, two different transfection protocols were compared, the BES-Calcium phosphate precipitation method and Lipofectamine 2000 transfection procedure (Invitrogen protocol). 10 μ g of pLenti6/V5-GW/lacZ (Invitrogen) expression vector were transfected in HEK 293T cells according to both protocols. 48 hours after transfection, the cells were stained with X-gal to check the expression of β -galactosidase (Fig.30). The BES-Calcium phosphate precipitation method was shown to be more effective than the Lipofectamine 2000 transfection procedure.

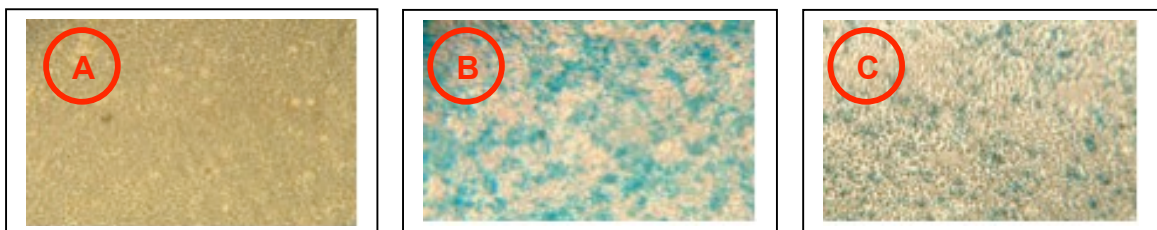


Figure 30: X-gal staining

A: HEK 293T cells, negative control; B: BES-Calcium Phosphate precipitation method; C: Lipofectamine 2000 transfection procedure

POTE2 γ was then cloned in an expression vector providing all the signals necessary for the expression of the gene in a mammalian cell line; the vector was pLenti6/V5-D-Topo (Invitrogen, Fig.31)

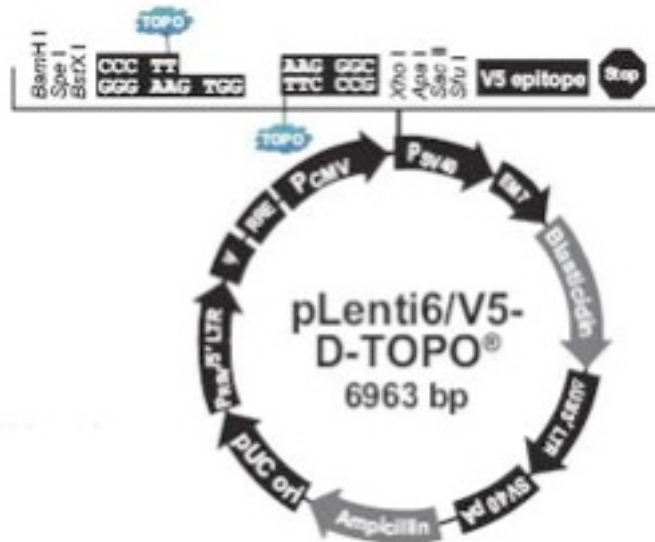


Figure 31: pLenti6/V5-Topo expression vector

To produce the lentiviral stock, 12 100mm-plates of 80% confluent HEK293T cells were cotransfected with 3 μ g of the expression vector and 9 μ g of Virapower Packaging Mix (Invitrogen, a mixture of 3 plasmids that provides *in trans* the structural and replicative proteins necessary for the viral packaging of the pLenti expression vector). After 18h, the transfection medium was replaced with 10 ml of fresh D-MEM medium + Sodium butyrate 10 mM³³ and, after further 24 hours, the viral supernatant was collected and concentrated.

The titre of POTE2 γ lentiviral stock in HT1080 cells was 9*10⁶ TU/ml (Fig. 32)

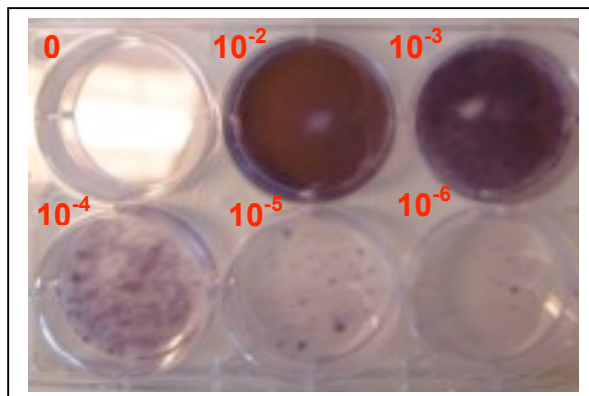


Figure 32: Titration of POTE2 γ lentiviral stock
Dilutions of the viral stock are reported in red.

2.2.2 POTE2 γ expression in MCF10A cells

POTE2 γ is expressed in many breast cancer cell lines; moreover, its expression is induced in normal breast epithelial cells transfected with oncogenes. These findings suggest that POTE2 γ expression is an event that occurs during

tumorigenesis. To evaluate the effect of POTE2 γ expression, it was decided to stably express this gene in a non-tumorigenic breast epithelial cell line, MCF10A (ATCC Number: CRL-10317).

To select for stably transduced cells, it was first necessary to perform a kill curve experiment, to determine the minimum concentration of Blasticidin required to kill untransduced cells within 10-14 days after antibiotic addition. For MCF10A cells, the minimum concentration was 6 μ g/ml.

MCF10A cells were infected with an MOI (Multiplicity Of Infection) of 1 and then selected. To confirm the integration of POTE2 γ into the genome of the selected cells, RT-PCR was performed. Two primers specific for POTE2 γ were used. The result was positive for Blasticidin selected MCF10A cells, where an amplification product of 386 bp was observable on agarose gel, in contrast to the negative result for wild-type MCF10A (Fig. 33).

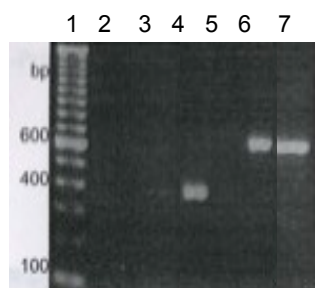


Figure 33 : RT-PCR

1, Ladder Marker; 2, Negative control, T444-T445 primers; 3, MCF10A cDNA, T444-T445 primers; 4, MCF10A/POTE2 γ cDNA, T444-T445; 5, Negative control, Actin primers; 6, MCF10A cDNA, Actin primers; 7, MCF10A/POTE2 γ cDNA, Actin primers

2.2.3 RNA interference

To further characterize the effect of POTE expression, it was decided to silence its expression using RNA interference (RNAi) combined with the lentiviral expression system.

RNAi is a phenomenon by which dsRNA induces a powerful and specific inhibition of eukaryotic gene expression via mRNA degradation, using short hairpin RNA (shRNA). shRNAs are an artificial class of RNAs that contain the following structural features: a short sequence of 19-29 nucleotides derived from the target gene, followed by a 4-15 nucleotides loop and then a reverse complement of the initial target sequence. When a specific shRNA is expressed in an eukaryotic cell line, mRNA of the target gene is degraded, silencing its expression. The lentivirus system was used to deliver the sequence coding for shRNA into the cells.

Initially, the silencing protocol was optimized for the target gene *lamin* (Genebank accession number: BC014507). A pair of complementary, single-strand DNA oligonucleotides, designed for *lamin* silencing (from Invitrogen), was synthesized and used with Invitrogen Block-it Lentiviral Expression System to generate the expression vector pLenti6/Block-It-shLam. this vector was employed to generate a lentiviral stock according to the procedure previously optimized. The titer of sh-lamin lentivirus was 5×10^7 TU/ml.

MCF7, a breast carcinoma cell line (ATCC Number: HTB-22), was chosen as the target cell line for *lamin* silencing. A kill curve experiment indicated 8 μ g/ml as the best Blasticidin concentration for selection of transduced cells. So, MCF7 cells were

infected with sh-lamin lentivirus at MOI=5 and selected. 10^7 wild-type and recombinant cells were lysed and analysed by Western Blotting (Fig.34).

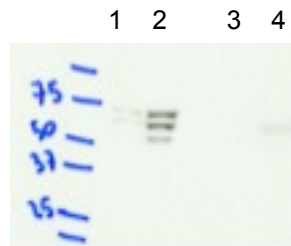


Figure 34: Western blot analysis of lamin silencing
1, MCF7 lysate, 10 μ g; 2, MCF7 lysate, 35 μ g; 3, MCF7-shLamin lysate, 10 μ g; 4, MCF7-shLamin lysate, 35 μ g

All three lamin variants are no longer expressed in sh-Lamin transduced cells, indicating that the gene was silenced.

Since the silencing of *lamin* in MCF7 using lentivirus as the delivery system of shRNA worked, sh-POTE lentivirus was prepared. A target sequence was identified with the help of Block-it RNAi Designer, a software provided by Invitrogen (Fig.35). Two complementary ss-DNA oligonucleotides containing the target sequence were prepared and used to produce sh-POTE lentivirus; the titre was $1,4 \times 10^6$.

¹ATGGTGGTTGAGGTTGATTCCATGCCGGCTGCCTCTTCTGTGAAGAAGCC⁵⁰
⁵¹ATTTGGTCTCAGGAGCAAGATGGGCAAGTGGTGCTGCCGTTGCTTCCCCT¹⁰⁰
¹⁰¹GCTACAGGGAGAGCGGC**AAGAGCAACGTGGGCACTTCT**TGGAGACCACGAC¹⁵¹

Figure 35: Target sequence for POTE2 γ silencing
Only the first 150 nucleotides of POTE coding sequence have been reported; target sequence for RNAi are in **red**.

3. CONCLUSIONS

Although several lines of evidence indicate that the PED-PLD1 interaction is involved in impairment of insulin-stimulated transport in type 2 diabetes, very little is known about this interaction.

In the present work, both PED and the D4 domain of PLD1, which is the shortest region still able to bind to PED, were cloned in a bacterial expression vector, expressed in *E. coli* and purified.

Hydrolysis in the presence of TEV protease enabled cleavage of PED from its fusion partners and its characterization. LC-MS of the entire protein and peptide mass fingerprinting confirmed its identity. PED α -helical structure resulted very stable, as seen with CD analysis and thermal denaturation.

Reducing conditions were used in all D4 manipulations, to avoid the formation of aggregates. Two different isoforms of D4, monomeric (D4M) and dimeric (D4D), were isolated. The intermolecular interaction in the dimeric form is not due to the formation of disulfide bonds, since reducing conditions were always employed. It is rather dependent on ionic strength, since at high saline concentration the equilibrium was shifted to the monomeric form.

Real-time BIA technology showed that PED only interacts with the monomeric form of D4; moreover, using trypsin-derived peptides in a competition assay, peptide 1-24 of PED resulted to be a strong competitor for D4 binding.

PLD dimerization is an event whose biological significance is unknown. PLD dimers might not be active: dimerization might hide the catalytic site of PLD, or dimers might be located at the wrong cellular site, because dimerization might occlude certain domains that specify localization of the monomer. Moreover, PLD domain(s) involved in this interaction have not been defined.

D4 is the C-terminal region of hPLD1 that contains one of the two HKD domains (the other is in the N-terminal region) whose dimerization is required for PLD activity^{16,17}. In the present study, it has been shown that D4 exists both as a monomer and dimer; these findings suggest that PLD might dimerize through an intermolecular interaction of D4 domains from two different PLDs. The result might be an inactive dimer, where the two N- and C-halves of each subunit do not interact to constitute the catalytic site.

PED only interacts with the monomeric form of D4. This might mean that *in vivo* PED binds the C-terminus of PLD1 during translation, stabilizing the active monomer and avoiding dimerization. Thus, in PED overexpressing cells, the concentration of the active monomeric form will be higher than in normal cells, resulting in higher PLD activity, and, subsequently, in impaired insulin-stimulated glucose transport.

Phosphorylation is not required for PED-PLD1 interaction, since PED-D4 binding was revealed with recombinant proteins expressed in bacteria. Using SPR technology to set up a competition assay, the D4-interacting region of PED has been identified. It consists of the first 24 amino acids of PED, corresponding to the first two helices of the DED. No phosphorylation site is present, and this explains why it is not involved in the PED-PLD1 interaction. Previous experiments localized the PED D4-binding site in region 53-112: from the competition assay, several peptides derived from this region competed with D4 for PED binding, but not as much as the 1-24 region.

Further experiments are ongoing to identify PED D4-binding site. Identification of these peptides implies several consequences. They can be used to model the PED-D4 interface, providing important insights in the elucidation of interaction details. They might be used *in vivo* to further characterize the effect of PED-D4 on glucose transport. Most importantly, these peptides might be used for pharmaceutical applications: block of PED-PLD in PED overexpressing cells might restore normal insulin-stimulated glucose transport.

Instead, the interest in POTE2 γ as a specific target in breast cancer therapies, has aroused interest in characterizing the effects of both its expression and its silencing.

The lentivirus system was used as vehicle for the generation of a stable POTE2 γ expressing cell line. A complete protocol for high throughput production of lentiviral stock was preliminarily set up, evaluating different cell transfection methods. MCF10A cells (a non-tumorigenic breast epithelial cell line) was infected with POTE2 γ recombinant lentiviruses to evaluate the effect of POTE expression in a breast cell line that doesn't express this gene. RT-PCR confirmed the insertion of this gene in the host cell line. Experiments are ongoing to analyze changes in gene expression by cDNA microarray

The lentiviral expression system was also found to be a powerful system for the expression of sh-RNA for gene silencing. It was able to efficiently silence a target gene, *lamin A/C*, in MCF7 cells (a breast cancer cell line). Recombinant sh-POTE2 γ lentiviruses were prepared, to evaluate the effect of POTE silencing in a cell line usually expressing this gene.

Anti-POTE antibodies have been prepared, and are currently being characterized. As soon as they become available, MCF7 cells will be infected with sh-POTE2 γ and the effect of silencing in the cell line will be evaluated.

4. EXPERIMENTAL PROCEDURES

4.1 MATERIALS AND INSTRUMENTS

PED and D4 cDNA and anti-PED rabbit serum were kindly provided by Prof. F. Beguinot, Dipartimento di Biologia e Patologia Cellulare e Molecolare, Università Federico II (Napoli, Italy). pETM vectors are from EMBL (Heidelberg, Germany). Oligonucleotides were synthesized by Sigma-Genosys (Sigma-Aldrich, Milano, Italy). Pfu DNA polymerase is from Stratagene (Milano, Italy). Restriction enzymes are from New England Biolabs (Milano, Italy). All molecular biology kits and Ni-NTA Magnetic Agarose Beads are from Qiagen (Milano, Italy). *Escherichia coli* bacterial strains are from Novagen (Milano, Italy), except for TOP10F' that are from Invitrogen (Milano, Italy). IPTG is from Inalco (Milano, Italy). Reagents for bacterial medium are from Becton-Dickenson (Milano, Italy). All reagents for native gels and SDS-PAGE, all chromatography columns and AKTA FPLC are from Pharmacia Amersham Biosciences (Milano, Italy). GAR-HRP antibody is from Bio-Rad (CA, USA); BIAcore system and reagents were from Pharmacia Biosensor AB (Uppsala, Sweden). All other reagents and chemicals are commercially available by Sigma-Aldrich or Fluka (Bucks, Switzerland).

Growth media for HEK293T, HT1080 and MCF7 cells (DMEM, Dulbecco's modified Eagle's medium+10 % FBS +1% Penicilin G sodium+2 mM L-glutamine) and for MCF10A cells (MEBM, Mammary Epithelium Basal Medium+MEGM Singlequots) are from Cambrex (AZ, USA). All Lentiviral vectors and reagents are from Invitrogen.

PCR Sprint is from Hybaid; all centrifuges are from Eppendorf (Milano, Italy), except for Allegra 6R and Avant J-25 centrifuges, from Beckman Coulter (Milano, Italy); UV/Visible spectrophotometer DU530 is from Beckman Coulter (Milano, Italy); bacterial incubators are from Infors Multitron; Sonicator 3000 is from Misonix; Microplate Reader Model 680 is from Biorad (CA, USA).

4.2 PED AND D4 CLONING

PED was PCR amplified with primers PEDFW (5'-CGCGCGCCATGGCTGAGTACGGGACCCTCCT-3') and PEDRV (5'-CGCGCGGATCCTTATCAGGCCTTCTTCGGTGGGGGAG-3'), using Pfu DNA polymerase and Tm=54°C. Amplified DNA was purified with QIAquick PCR Purification Kit and digested with NcoI, again purified with QIAquick PCR Purification Kit and then digested with BamHI enzyme. Double digested fragment was extracted from 1,2% agarose gel using QIAquick Gel Extraction KIT and ligated into pETM vectors, previously digested and dephosphorylated. Ligation products were electroporated into TOP10F' and recombinant colonies were selected by PCR; expression vectors from positive clones were isolated using QIAprepSpin Miniprep kit.

D4 was PCR amplified with primers D4FW (5'-GCGCGCGAAGACCCATGGG GTCCCTTTCTTATCCTTTTCTGCTT-3') and D4RV (5'-CGCGCGCTCGAGTCATTA TTAAGTCCAAACCTCCATGGGCACTATG-3') and then double digested with BbsI and XhoI enzymes. Recombinant expression vectors were isolated as described for PED expression vectors.

4.3 PED AND D4 EXPRESSION SCREENING

100 ng of expression vector were chemically transformed in competent cells. Two colonies were grown in LB medium o/n at 37°C, then diluted to 0,06 OD/ml and induced with IPTG when the culture was grown to 0,6 OD/ml. After 16h at 22°C, 1,5

ml of bacterial culture was harvested, lysed and purified on Ni-NTA Magnetic Agarose Beads (following QIAGEN protocol). Magnetic beads are resuspended in 10 μ l of SDS-Loading buffer (Tris-HCl 50 mM, SDS 1%, blue bromophenol 0.1%, glycerol 10%, pH 6.8) and analyzed on SDS-PAGE together with 10 μ l of total and soluble fractions of the lysates.

A first screening was done by transforming all 5 pETM expression vectors (see Table 1) in BI21(DE3) cells, and inducing with 1 mM IPTG. After having chosen the best expression vector, results with different *E. coli* strains were evaluated (BI21(DE3)pLysS, Rosetta(DE3), Rosetta(DE3)pLysS, C41(DE3), C43(DE3), BI21star (DE3), BI21star(DE3)pLysS, BI21(DE3)RIP, BI21(DE3)RIL) and optimal concentration of IPTG was determined.

For PED, a further experiment showed that the yield was the same by inducing 16 h at 22°C or 3h at 37°C.

4.4 PED PURIFICATION

100 ml of bacterial culture were resuspended in 4 ml of Phosphate buffer 20 mM, NaCl 500mM, PMSF 1mM, Triton 0.05%, Lysozyme 1 μ g/ml, pH7.4, left for 30' at RT and then sonicated for 2 minutes (20'' on, 10'' off). Lysate was then centrifuged for 20' at 4°C at 18 krpm and the soluble fraction was loaded on a His-trap Column, previously equilibrated with Buffer A (Sodium-phosphate buffer 20 mM, NaCl 500mM, pH7.4). PED+Gst+His6 was purified with the following protocol:

	CV	% BUFFER B (Buffer A + Imidazole 500mM, pH 7.4)
WASH	15	12
ELUTION	5	60

Purified protein was dialysed against Phosphate buffer 20 mM, NaCl 150mM, pH 7.4 and hydrolysed in the presence of 0,01 mg TEV protease (expressed and purified in our laboratories) for each mg of PED, DTT 1mM, EDTA 0,5mM, for 16 h at 30°C.

Digested PED was loaded on a His-trap Column, previously equilibrated in Sodium phosphate buffer 20 mM, NaCl 150mM, pH 7,4, and PED was recovered in the flow-through.

If necessary, PED was further loaded on a Gst-trap column, recovered in the flow-through, dialysed against Tris-HCl 20 mM, pH 7,5 (Buffer C) and eventually purified on a MonoQ column:

	CV	% BUFFER D (Tris-HCl 50 mM, NaCl 1M, pH 7,5)
WASH	2	0
GRADIENT	10	0 to 50%

PED was eluted at 7% B (70 mM NaCl).

4.5 D4 PURIFICATION

200 ml of bacterial pellet was lysed in 20 ml of Tris-HCl 50 mM, NaCl 200 mM, Imidazole 20 mM, PMSF 1 mM, Triton X-100 0,25%, Lysozyme 1 μ g/ml, TCEP 1 mM, pH 7,5 for 30' at RT. Then, it was sonicated for 6 minutes (20'' on, 20'' off), centrifuged 20' at 4°C at 15 krpm. The soluble fraction was loaded on a His-trap column and purified according to the following protocol:

BUFFER 1: Tris-HCl 50 mM, NaCl 200 mM, Imidazole 20 mM, TCEP 1 mM, pH 7,5
BUFFER 2: Tris-HCl 50 mM, NaCl 200 mM, Imidazole 500 mM, TCEP 1 mM, pH 7,5

	CV	% BUFFER 2
WASH	10	0
ELUTION	5	36

2 ml of D4+TrxA+His6 from His-trap were diluted with 18 ml of Buffer 3 (Tris-HCl 50 mM, TCEP 1 mM, pH 7,5), loaded on a MonoQ column and purified according to the the following protocol:

	CV	% BUFFER 4 (Tris-HCl 50 mM, NaCl 1 M, TCEP 1 mM, pH 7,5)
WASH	5	0
ELUTION	20	0 to100

D4M and D4D were separated using a Superdex200 column, in TrisHCl 50 mM, NaCl 250 mM, TCEP 1 mM, pH 7,5.

4.6 PED AND D4 CHARACTERIZATIONS

LC-MS was performed using 5 µl of a 0.1 mg/ml sample and a LCQ DCA XP Ion Trap spectrometer (ThermoElectron, Milan, Italy). This was equipped on OPTON ESI source (operating at a needle voltage of 4.2 kV and a temperature of 320 °C) and a complete Surveyor HPLC system (including a MS pump, an autosampler and a photo diode array [PDA]). Analyses were performed using a narrow bore 250x2 mm C4 Jupiter column, 300 Å, 3 µm (Phenomenex) and eluting with H₂O/0.08%TFA (A) and CH₃CN/0.05% TFA (B) gradients:

TIME (min)	% B
0	30
6	30
35	70
36	95
41	95
42	30

During this time, the sample tray was kept at 20°C, whereas the column was kept at 25°C. Mass spectra were recorded continuously at mass intervals of 400-2000 amu in positive mode (LC-MS, condition 1). Multicharge spectra were then deconvoluted using the BioMass program implemented in the Bioworks 3.1 package provided by the manufacturer. Mass calibration was performed automatically by means of selected multiple charged ions, in the presence of a calibrant (Ultramark, ThermoElectron). All masses were reported as average values.

PED proteolysis was performed by incubation with TPCK-treated trypsin (Sigma-aldrich, Milan) at an enzyme:substrate ratio of 1:100 in 50 mM Tris-HCl pH7.5. LC-MS was performed as previously described, eluting with H₂O/0.08%TFA (A) and CH₃CN/0.05% TFA (B) gradient:

TIME (min)	% B
0	5
3	5
68	70
70	90
80	90
82	5
90	5

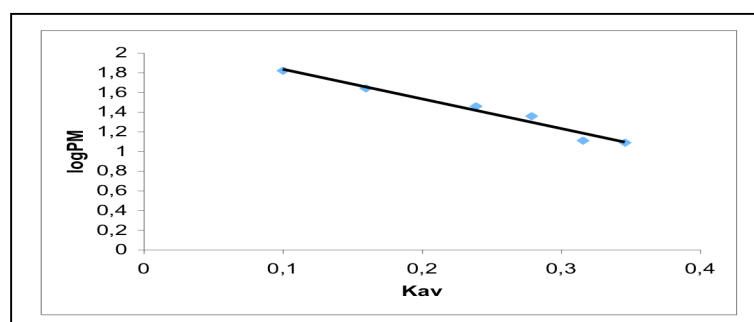
Mass spectra were recorded continuously at mass intervals of 400-2000 amu, in positive mode and Data-Dependent Analysis (DDA) in order to fragment the eluted peptides and obtain sequence information. Fragmentation was induced on selected ions from 400 to 1200 amu, with a fixed 35% of total radio-frequency energy.

CD spectra were obtained on a Jasco J-715 dichrograph, calibrated at 290 nm with an aqueous solution of D(+)-10-canphor sulphonic acid. Data were collected at 0.2 nm intervals with a 20 nm min⁻¹ scan speed, a 2 nm bandwidth and a 16 s response, from 260 to 190 nm.

4.7 SUPERDEX75 AND SUPERDEX200 CALIBRATIONS

Superdex75 column was calibrated using the following standard proteins in Sodium-phosphate buffer 20 mM, NaCl 150mM, pH 7.5 (V₀ is 7,7 ml; V_t is 24 ml):

PROTEIN	MOLECULAR WEIGHT (kDa)	logMW	ELUTION VOLUME (V _e , ml)	K _{av} (V _e -V ₀)/V _t -V ₀)
BSA	66	1,82	9,3	0,1
OVALBUMIN	44	1,64	10,3	0,159
CARBONIC ANIDRASE	29	1,46	11,6	0,239
CHYMOTRYPSINOGEN	23	1,36	12,3	0,279
RIBONUCLEASE	13	1,11	12,9	0,315
C CYTOCHROM	12,4	1,09	13,4	0,346



The resulting calibration curve is $y = -3,02x + 2,13$ ($R^2 = 0,97$).

For Superdex200, the following standards were run in Sodium-phosphate buffer 20 mM, NaCl 150mM, pH 7,5 (V₀ is 7,1 ml; V_t is 24 ml):

PROTEIN	MOLECULAR WEIGHT (kDa)	logMW	ELUTION VOLUME (V _e , ml)	K _{av} (V _e -V ₀)/V _t -V ₀)
FERRITINE	460	2,66	9,7	0,154
CATALASE	206	2,31	11,5	0,262
ALDOLASE	170	2,23	11,9	0,283
TRANSFERRIN	81	1,91	12,9	0,343
BSA	66	1,82	13	0,347

OVALBUMIN	43	1,64	14,1	0,415
CARBONIC ANIDRASE	29	1,46	15,4	0,489
C CYTOCHROM	12,4	1,09	16,8	0,574

The resulting calibration curve is $y = -3,76x + 3,24$ ($R^2 = 0,99$).

4.8 ELISA ASSAYS

To dose anti-PED serum, PED solutions at different concentrations were used to coat microtitre wells for 1h at 37°C. The wells were then blocked for 1 h at 37°C with 1% BSA in PBS. Different dilutions of anti-PED rabbit serum were added and incubated for 1h at 37°C. Interaction was revealed by adding 1:5000 GAR-HRP antibodies (1h at 37°C) and staining with Sigma Fast. Each passage was followed by an extensive wash with PBS+0,2% Tween20.

To detect PED-D4 interaction, different concentrations of D4+TrxA+His6 solutions in PBS were coated on the wells over night at 4°C; after an extensive wash with PBS+0,2% Tween 20, the wells were blocked with 1% BSA in PBS for 1 h at 37°C. After washing, increasingly concentrated solutions of PED were added and incubated for 1h at 37°C. After washing, 1:10000 dilution in PBS of anti-PED rabbit serum were added and the plate was left for 1h at 37°C. GAR-HRP was used for revelation as previously described.

4.9 PED COATING ON SENSOR SURFACE

A CM5 sensor chip was used to bind PED using the standard amine coupling procedure as described by the manufacturer's instructions. 30 µl of a N-hydroxy-succinimide and N-ethyl-N'-(dimethyl-aminopropyl)-carbodiimide mixture were injected at a flow rate of 5 µl/min to activate the sensor surface, followed by 30, 25 and 15 µl injections of PED diluted to 0,1 mg/ml in acetate buffer pH 4.0. Unreacted activated groups were blocked by a 15 µl injection of ethanolamine.

Binding assays were carried at a flow rate of 30 µl/min.

4.10 PREPARATION OF PED PEPTIDES

PED was hydrolyzed using 1:100=enzyme:substrate of TPCK-treated Trypsin (Sigma-Aldrich, Milan), 16h at 37°C.

Preparative RP-HPLC were carried out on a Shimadzu LC-8A, equipped with a SPD-M10 AV detector on a Phenomenex Jupiter C₁₈ column (1 × 25 cm; 10 µm) with H₂O/0.1%TFA (A) and CH₃CN/0.1% TFA (B). The gradient used for purification was 5 to 70% B in 60min, at a flow rate of 4 ml/min.

LC-MS of pools was performed as previously described, using gradients:

Pools F-1-2-3	
TIME (min)	% B
0	1
5	1
40	30
43	95
48	95
49	1
54	1

Pools 4-5-6	
TIME (min)	% B
0	5
3	5
33	65
35	95
40	95
41	5
45	5

4.11 HEK293T CELL TRANSFECTION WITH pLenti6/V5-GW/lacZ

Poly-lysine precoated plates were each seeded with 3×10^6 HEK293T cells and cultured with 10 ml of fresh growth media at 37°C, 5% CO₂. After 16 h, 10 µg of DNA were diluted to a final volume of 450 µl with sterile TE buffer (10 mM Tris-HCl pH 8.0+1mM EDTA). 50 µl of 2.5 M CaCl₂ was added and solution was mixed. The 500 µl of DNA solution were slowly added to 500 µl of 2X BBS (BES-Buffered Saline 2X: NaCl 280 mM; Na₂HPO₄ 1.5 mM; BES 50 mM, pH 6.95). Incubation at RT for 15' allowed the Calcium Phosphate –DNA complex to form. The calcium Phosphate-DNA mixture was added drop-wise to cultured cells and incubated at 37°C, 3% CO₂. After a further 16h, the transfection medium was removed and 10 ml of fresh growth medium were added and left at 37°C, 5% CO₂. After 24 h, cells were checked for expression.

4.12 X-GAL STAINING

Cells were washed with PBS and then 4% formic acid in PBS was added. After 20' at RT, 2 ml of X-gal solution (Potassium Ferricyanide 5mM, Potassium Ferrocyanide 5mM, 1mM MgCl₂, x-gal 500 µg/ml, in PBS) were added. The stain was visible after 2 h at 37°C.

4.13 CRYSTAL VIOLET STAINING FOR BLASTICIDIN RESISTANT COLONIES

Cells were washed with PBS and fixed in 10% Neutral Buffered Solution for 30'. Cells were washed again with PBS, 1% Crystal Violet was added and, after 30' at RT, cells were washed with PBS until PBS is clear.

4.14 VIRUS PRODUCTION

12 poly-lysine precoated 100mm-plate were each seeded with 3×10^6 HEK293T cells and cultured with 10 ml of fresh growth media at 37°C, 5% CO₂, o/n. Cells should be 70-80% confluent and evenly distributed at the time of transfection. For each plate, 3 µg of expression plasmid were mixed with 9 µl of Virapower Packaging Mix and diluted to a final volume of 450 µl with sterile TE buffer (10 mM Tris pH 8.0+1mM EDTA). 50 µl of 2.5 M CaCl₂ was added and mixed. The 500 µl of DNA solution was slowly added to 500 µl of BBS 2X (BES-Buffered Saline 2X: NaCl 280 mM; Na₂HPO₄ 1.5 mM; BES 50 mM, pH 6.95) and after 15 min the mixture was added drop-wise to cultured cells and incubated at 37°C, 3% CO₂. After 16 h, the transfection medium was removed and 10 ml of fresh growth medium+100 µl of Sodium butyrate 1M (final concentration 10 mM) were added. After a further 16 h at 37°C, 5% CO₂, the viral supernatant was harvested, centrifuged at 1000 rpm for 3 min and passed through a 0.45 µm filter. Filtered supernatant was concentrated at 26 krpm for 2.5 hrs at 20°C. Viral pellets were resuspended in 1 ml of PBS. Viral stocks were frozen in aliquots at -80°C.

4.15 LENTIVIRAL STOCK TITRATION

Each well of a 6-well plate was seeded with 2×10^5 HT1080 cells in 2 ml of growth medium and incubated o/n, 37°C, 5% CO₂. Next day, 10-fold serial dilutions, ranging from 10⁻² to 10⁻⁷, of the lentiviral stock solution were prepared into growth medium to a final volume of 1 ml. Medium from the cells was removed and, after mixing, each dilution was added to one well of cells. After 16 h at 37°C, 5% CO₂, the

media containing virus was removed and replaced with 2 ml of fresh growth medium. The following day, the medium was exchanged with fresh medium + 4 µg/ml Blasticidin; then, every 2-3 days, medium was changed with fresh medium + Blasticidin. After 10-12 days of selection, the cells were stained with Crystal violet solution.

4.16 RT-PCR

RNA was extracted from 10^6 cells with 1ml of TRIzol reagent (Gibco BRL) and resuspended in 10 µl of dH₂O. 11 µl were used to synthesize cDNA using First-Strand cDNA Synthesis Kit (Amersham Biosciences). 2 µl were used for a PCR reaction with oligonucleotides T444 (5'-CAA TGC CAG GAA GAT GAA TGT GCG-3') and T445 (5'-TCT CTG GCC GTC TGT CCA GAT AGAT-3'), T_m=65°C. Actin amplification was used as positive control.

4.17 WESTERN BLOT

10^7 cells were suspended in 400 µl of Tris-HCl 50 mM, PMSF 1 mM, 4 µg/ml Aprotinin, pH7.4 and sonicated for 2'(10" on, 10" off). Then 20 µl of Tris-HCl 50 mM, DNase 1 mg/ml, RNase 250 µg/ml, MgCl₂ 50 mM, pH 7.5 were added and, after 30' at RT, 50 µl of TCA were added. After 20' incubation on ice, lysate was centrifuged at 1500 rpm at 4°C for 10', supernatant was removed and the pellet was washed twice with 1 ml of Acetone. The pellet was resuspended in 320 µl of Urea 9M, Triton-X100 2%, β-mercaptoethanol 5%, then 80 µl of 10% LDS and 0,1 % BPB were added. Samples were run on SDS-PAGE and then transferred to a PVDF membrane for 4 h at 30V at 4°C with constant stirring. The membrane was blocked for 16 h at 4°C with 1% Western Blocking Reagent (Roche) in TBS (Tris-HCl 50 mM, NaCl 150 mM, pH 7.5), then incubated with 1:1000 dilution in TBS of Purified Mouse Anti-lamin A/C Mouse Antibody (BD Transduction Laboratories). The membrane was then washed twice with TBST (TBS+0.1 % Tween20) and twice with 0.5% Western Blocking Reagent in TBS. 1:30 dilution of Alp-goat Anti Mouse IgG's in TBS+0.5% Western Blocking Reagent was added and, after 1 h at RT, the membrane was extensively washed with TBST. 1-step NBT/BCIP solution was used to stain the membrane.

4. ABBREVIATIONS

β-MERCAPOTETHANOL	2-mercaptoethanol
ATCC	American Type Culture Collection
BES	N,N-Bis(2-hydroxyethyl)-2-aminoethanesulfonic acid
BP	Base Pair
BSA	Bovine Serum Albumin
CD	Circular Dichroism
cDNA	Complementary DNA
CV	Column Volume
D4D	Dimeric D4
D4M	Monomeric D4
DAG	Diacylglycerol
DED	Death Effector Domain
D-MEM	Dulbecco's Modified Eagle Medium
DNA	Deoxyribonucleic Acid
DNAse	Deoxyribonuclease
dsRNA	Double Stranded RNA
EDTA	Ethylenediaminetetraacetic Acid
EST	Expressed Sequence Tag
FBS	Fetal Bovin Serum
FPLC	Fast Protein Liquid Chromatography
GAR-HRP	Goat- Anti Rabbit Horseradish Peroxidase
GST	Glutathion S-transferase
HBS	0.01 M HEPES, pH 7.4, 0.15 M NaCl, 3 mM EDTA, 0.005% Surfactant P20
His	Histidin
HIV	Human Immunodeficiency Virus
IPTG	Isopropyl-b-D-Thiogalactopyranoside
lacZ	β-galactosidase
LB	Bacto-triptone 10 g/l, Yeast Extract 5 g/l, NaCl 10 g/l
LC-MS	Liquid Chromatography- Mass Spectrometry
MOI	Multiplicity Of Infection
NMR	Nuclear Magnetic Resonance

O.D.	Optical Density
ORF	Open Reading Frame
PBS	Phosphate-Buffered Saline Buffer
PCR	Polymerase Chain Reaction
PEA15	Phosphoprotein Expressed in Astrocytes 15
PED	Phosphoprotein Enriched in Diabetes
PKC	Protein Kinase C
PLD1	Phospholipase 1
PMSF	Phenylmethylsulphonylfluoride
POTE	Prostate, Ovary, Testis Expressed gene
PVDF	PolyVinylidene DiFluoride
RNA	Ribonucleic Acid
RNAi	RNA interference
RNAse	Ribonuclease
RP-HPLC:	Reverse Phase-High Performance Liquid Chromatography
RT	Room Temperature
RT-PCR	Reverse Transcriptase-Polymerase Chain Reaction
RU	Reflecting Units
SDS	Dodecylsulphate Sodium
shRNA	Short Hairpin RNA
SPR	Surface Plasmon Resonance
TBS	TrisHCl 50 mM, NaCl 150 mM, pH 7.5
TBST	TBS+0.1 % Tween20
TCEP	Tris(2-carboxyethyl)phosphine hydrochloride
TEV	Tobacco Etch Virus
TFA	Trifluoroacetic Acid
Tris-HCl	2-Amino-2-(hydroxymethyl)-1,3-propanediol, hydrochloride
TrxA	ThioredoxinA

5. REFERENCES

- 1- Higgins and Hames (1999). Protein Expression, Oxford University Press
- 2- Condorelli G., Trecia A., Vigliotta G., Perfetti A., Goglia U., Cassese A., Musti A.M., Miele C., Santopietro S., Formisano P., Beguinot F. (2002). Multiple members of the mitogen-activated protein kinase family are necessary for PED/PEA15 anti-apoptotic function. *The Journal of Biological Chemistry* 277(13):11013-11018
- 3- Krueger J., Chou F.-L., Glading A., Schaefer E., Ginsberg M.H. (2005). Phosphorylation of phosphoprotein enriched in astrocytes (PEA-15) regulates extracellular signal-regulated kinase-dependent transcription and cell proliferation. *Molecular Biology of the Cell* 16:3552-3561
- 4- Xiao C., Yang B. F., Asadi N., Beguinot F., Hao C. (2002). Tumor necrosis factor-related apoptosis-inducing signaling complex and its modulation by c-Flip and PED/PEA-15 in glioma cells. *The Journal of Biological Chemistry* 28(227):25020-2502
- 5- Arajou H., Danziger N., Cordier J., Glowinski J., Chneiweiss H. (1993). Characterization of PEA-15, a major substrate for Protein Kinase C in astrocytes. *The Journal of Biological Chemistry*, 268(8): 5911-5920
- 6- Hill J.M., Vaidyanathan H., Ramos J.W., Ginsberg M.H., Werner M.H. (2002). Recognition of ERK MAP kinase by PEA-15 reveals a common docking site within the death domain and death effector domain. *The EMBO Journal* 21(23): 6494-6504
- 7- Kubes M, Cordier J., Glowinski J., Girault A., Chneiweiss H. (1998). Endothelin induces a calcium-dependent phosphorylation of PEA-15 in intact astrocytes: identification of Ser104 and Ser116 phosphorylated, respectively, by protein kinase C and calcium/calmodulin kinase II in vitro. *Journal Neurochem.* 71:1303-1314
- 8- Trecia A., Perfetti A., Cassese A., Vigliotta G., Miele C., Santopietro S., Oriente F., Santopietro S., Giacco F., Condorelli G., Formisano P., Beguinot F (2003). Protein kinase B/Akt binds and phosphorylates PED/PEA-15 stabilizing its antiapoptotic action. *Molecular and Cellular Biology* 23(13): 4511-4521
- 9- Condorelli G., Vigliotta G, Iavarone C., Caruso M., Tocchetti C.G., Andreozzi F., Cafieri A., Tecce M.F., Formisano P., Beguinot L., Beguinot F. (1998) PED/PEA-15 gene controls glucose transport and is overexpressed in type 2 diabetes mellitus. *The EMBO Journal* 17(14): 3858-3866
- 10-Vigliotta G., Miele C., Santopietro S., Portella G., Perfetti A., Maitan M.A., Cassese A., Oriente F., Trecia A., Fiory F., Romano C., Tiveron C., Tatangelo L., Formisano P., Beguinot F. (2004). Overexpression of the *ped/pea-15* gene causes diabetes by impairing glucose-stimulated insulin secretion in addition to insulin action. *Molecular and Cellular Biology* 24(11):5005-5015
- 11-De Fronzo R.A. (1995). Pathogenesis of type 2 diabetes: metabolic and molecular implications for identifying diabetes genes. *Diabetes Rev.* 5:177-269
- 12-Kahn C.R. (1994). Insulin action, diabetogenesis and the cause of type 2 diabetes. *Diabetes* 43:1066-1084
- 13-Condorelli G., Vigliotta G., Trecia A., Maitan M.A., Caruso M., Miele C., Oriente F., Santopietro S., Formisano P., Beguinot F. (2001). Protein kinase C(PKC)- α activation inhibits PKC- ζ and mediates the action of PED/PEA15 on glucose transport in the L6 skeletal muscle cells. *Diabetes* 50:1244-1252

- 14-Zhang Y., Redina O., Altshuller Y.M., Yamazaki M., Ramos J., Chneiweiss, Kanaho Y., Frohman M.A. (2000). Regulation of expression of Phospholipase D1 and D2 by PEA-15, a novel protein that interacts with them. *The Journal of Biological Chemistry* 275(45):35224-35232
- 15-McDermott M., Wakelam M.J.O., Morris A.J. (2004). Phospholipase D^{1,2}. *Biochem. Cell. Biol.* 82:225-253
- 16-Xie Z., Ho W-T, Exton J. (2000). Association of the N- and C-terminal domains of Phospholipase D. *The Journal of Biological Chemistry* 275(32):24962-24969
- 17-Xie Z., Ho W-T, Exton J. (1998). Association of the N- and C-terminal domains of Phospholipase D is required for catalytic activity. *The Journal of Biological Chemistry* 273(52):34679-34682
- 18- Kam Y., Exton J.H. (2002). Dimerization of Phospholipase D isozymes. *Biochemical and Biophysical Research Communication* 290:375-380
- 19-Besterman J.M, Duronio V., Cuatrecasa P. (1986). Rapid formation of diacylglycerol from phosphatidylcholine: a pathway for generation of a second messenger. *Proc. Natl. Acad. Sci. USA* 83:6785-6789
- 20-Nesher R., Anteby E., Yedovizky M., Warwar N., Kaiser N., Cerasi E. (2002). Beta-cell protein kinases and the dynamics of the insulin response to glucose. *Diabetes* 51(1):S68-73
- 21-Sung T.C., Zhang Y., Morris A.J., Frohman M.A. (1999). Structural analysis of human phospholipase D1. *The Journal of Biological Chemistry* 274(6):3659-3666
- 22-Karolewski B.A, Watson D.J., Parente M.K., Wolfe J.H. (2003) Comparison of transfection conditions for a lentivirus vector produced in large volumes. *Human Gene Therapy* 14:1287-1296
- 23-Yamazaki M., Zhang Y., Watanabe H., Yokozeki T., Ohono S., Kaibuchi K., Shibata H., Mukai H., Ono Y., Frohman M.A., Kanaho Y. (1999). Interaction of the small G protein RhoA with the C-terminus of human phospholipase D1. *The Journal of Biological Chemistry* 274(10):6035-6038
- 24-Du G., Altshuller Y.M., Kim Y., Han J.M., Ryu S.H., Morris A.J., Frohman M.A. (2000). Dual requirement for Rho and Protein Kinase C in direct activation of phospholipase D1 through G protein-coupled receptor signaling. *Molecular Biology of the Cell* 11:4359-4368
- 25-Fagerstam L.G., Frostell-Karlsson A., Karlsson R., Persson B., Ronnberg I. (1992). Biospecific interaction analysis using SPR detection applied to kinetic binding site and concentration analysis. *Journal of Chromatography* 597:397-410
- 26- Altschuh D., Dubs M.C., Weiss E., Zeder-Lutz G., Van Regenmortel M.H.V. (1992). Determination of kinetic constants for the interaction between a monoclonal antibody and peptides using SPR. *Biochemistry* 31:6298-63104
- 27-Schuck P. (1997). Use of SPR resonance to probe the equilibrium and dynamic aspects of interactions between biological macromolecules. *Ann. Rev. Biophys. Biomol. Struct.* 26:541-566
- 28-Johnsson B., Lofas S., Lindquist G. (1991). Immobilization of proteins to a carboxymethyl dextran modified gold surface for biospecific interaction analysis in SPR sensors. *Anal. Biochem.* 198:268-277
- 29-International Human Sequencing Consortium (2001). *Nature* 409:860-920
- 30- Vasmataz G., Essand M., Brinkmann U., Lee B., Pastan I. (1998). Discovery of three genes specifically expressed in human prostate by expressed sequence tag database analysis. *Proc. Natl. Acad. Sci. USA* 95:300-304
- 31-Bera T.K., Zimonjic D.B., Popescu N.C., Sathyanarayana B.K., Kumar V., Lee B., Pastan I. (2002). *POTE*, a highly homologous gene family located on numerous

- chromosomes and expressed in prostate, ovary, testis, placenta, and prostate cancer. *PNAs* 99(26): 16975-16980
- 32- Bera T.K., Huynh N., Maeda H., Sathyanarayana B.K., Lee B., Pastan I. (2004). Five POTE paralogs and their splice variants are expressed in human prostate and encode proteins of different lengths. *Gene* 337:45-53
- 33- Bera T.K., Saint Fleur A., Lee Y., Kydd A., Hahn Y., Popescu N.C., Zimonjic D.B., Lee B., Pastan I. (2006). POTE paralogs are induced and differentially expressed in many cancers. *Cancer Res*, 66(1):52-6
- 34- Dull T., Zufferey R., Kelly M., Mandel R.J., Nguyen M., Trono D., Naldini L. (1998). A third-generation lentivirus vector with a conditional packaging system. *Journal of Virology*, 72: 8463-8471
- 35- Zufferey R., Dull T., Mandel R.J., Bukovsky A., Quiroz D., Naldini L., Trono D. (1998). Self-inactivating lentivirus for safe and efficient *in vivo* gene delivery. *Journal of Virology* 72:9873-9880
- 36- www.embl-heidelberg.de/ExternalInfo/protein_unit/draft_frames/flowchart/clo_vector/our_Ec_vectors.html

CONGRESS COMMUNICATIONS

Francesca Viparelli, Nunzianna Doti, Annamaria Sandomenico, Simona M. Monti, Nina Dathan, Laura Tornatore, Maddalena Pizzulo, Mariano Amoroso, Francesco Beguinot, Claudia Miele, Daniela Marasco, Ettore Benedetti, Carlo Pedone, Menotti Ruvo. PED binds with high affinity to the D4 domain of PLD1. *10th Naples Workshop on Bioactive Peptides, 2006.*

Introduction: PED/PEA (Phosphoprotein Enriched in Diabetes or in Astrocytes) or PED is a ubiquitously expressed 15 kDa cytosolic protein with recognized multiple functions. It has been indeed demonstrated that PED has broad proapoptotic properties (1) and, by altering insulin secretion, has a proven implication in diabetes (2). In cultured cells and in transgenic mice, PED overexpression induces insulin-resistance and impairs glucose tolerance. Recent evidence indicates that increased interaction of PED with Phospholipase D1 (PLD1) is a key event leading to these abnormalities in vivo and that this interaction is mediated by a large, C-terminal domain of PLD1 comprising residues 712-1070 (3). We have prepared PED and a D4-fusion protein containing thioredoxin (Trx) at the N-terminal side to investigate protein structures and to set up a binding assay for the screening of potential antagonists. The two proteins have been purified and refolded and the recognition properties have been characterized by ELISA assays and by Surface Plasmon Resonance.

Result and Discussion: ped was cloned in a pETM30 vector and expressed in a BL21(DE3)star E.coli strain. Expression gave very high levels of the fusion protein GST-His6-PED. After a first step of purification on a His-trap column, the GST-His6 portion was cleaved and PED purified using again a His-trap column followed by a further anion exchange step on a MonoQ column. Mass spectrometry analysis of the entire and trypsin-treated protein confirmed protein identity, whereas a characterization by CD spectroscopy showed, as expected, that the protein had an all-alpha secondary structure (4). D4 was cloned in several vectors with different tags and several strains of E. coli were tested to optimize the expression of the fusion protein (MW about 56 kDa). Optimal results were achieved using the pETM20 vector in the BL21(DE3)pLysS strain. Preliminary purification attempts of the resulting protein, Trx-His6-D4, gave poorly reproducible results, likely due to aggregation events associated to the high number of cysteines in the D4 domain. Remarkable improvements were achieved by carrying out the purification in a TCEP-containing buffer (1 mM). The fusion protein was then purified on a His-trap column, followed by an anionic exchange chromatography step. Attempts to cleave the tag protein with TEV protease were unfruitful, as the amount of cut protein was invariably very low. The fusion protein was therefore used in binding experiments with purified PED. Preliminary ELISA assays confirmed the binding of PED to Trx-His6-D4 and the lack of any interference by the Trx tag. Further binding experiments, carried out with Biacore3000, allowed the determination of the kinetic parameters and an evaluation of the dissociation constant that was estimated to be $2 \pm 1 \times 10^{-7} \text{ M}^{-1}$.

References

1. Protein kinase B/Akt binds and phosphorylates PED/PEA-15, stabilizing its antiapoptotic action. Trecia A, Perfetti A, Cassese A, Vigliotta G, Miele C, Oriente F, Santopietro S, Giacco F, Condorelli G, Formisano P, Beguinot F. *Mol Cell Biol* 2003 Jul;23(13):4511-21.
2. Overexpression of the ped/pea-15 gene causes diabetes by impairing glucose-stimulated insulin secretion in addition to insulin action. Vigliotta G, Miele C, Santopietro S, Portella G, Perfetti A, Maitan MA, Cassese A, Oriente F, Trecia A, Fiory F, Romano C, Tiveron C, Tatangelo L, Troncone G, Formisano P, Beguinot F. *Mol Cell Biol* 2004 Jun;24(11):5005-15.

3. Regulation of expression of phospholipase D1 and D2 by PEA-15, a novel protein that interacts with them. Zhang Y, Redina O, Altshuler YM, Yamazaki M, Ramos J, Chneiweiss H, Kanaho Y, Frohman MA. *J Biol Chem*. 2000 Nov 10;275(45):35224-32.
4. Recognition of ERK MAP kinase by PEA-15 reveals a common docking site within the death domain and death effector domain. Hill JM, Vaidyanathan H, Ramos JW, Ginsberg MH, Wemer MH. *EMBO J*. 2002 Dec 2;21(23):6494-504.

Laura Tornatore, Simona M. Monti, Nina Dathan, Annamaria Sandomenico, Daniela Marasco, Nunzianna Doti, Francesca Viparelli, Maddalena Pizzulo, Mariano Amoroso, Ettore Benedetti, Carlo Pedone, Menotti Ruvo. Expression, purification and characterization of Gadd45 β . *10th Naples Workshop on Bioactive Peptides, 2006*.

Introduction: The Gadd45 family of proteins is involved in a wealth of cellular events. They are key mediators of cell cycle arrest, apoptosis, signal transduction and cell survival, often stimulating opposite signals depending on cell types and/or status. Gadd45 β , as an example, prevents apoptotic cell death in response to TNF α (De Smaele, Zazzeroni et al. 2001), whereas it can also favour apoptosis following TGF β stimulation (Lu, Ferrandino et al. 2004). Despite the increasing interest around this protein class, little is known about their structural organization. As it has been demonstrated that Gadd45 α is able to self associate in small oligomers that can have a role in protein functionality (Kovalsky, Lung et al. 2001), we have investigated such aspects in human Gadd45 β . To this aim, the protein has been prepared, purified and refolded and a preliminary structural characterization by CD has also been carried out.

Result and Discussion: Initial expression and purification experiments were all performed with the original pET28aGADD45 β clone. However, although the purification appeared to work well, when samples were electrophorated under non-denaturing conditions following gel filtration GADD45 β appeared to run as a dimer, trimer or even higher form of oligomers. Although GADD45 α reportedly exists predominantly as a dimer (Kovalsky et al, 2001), there exists no evidence as yet that GADD45 β also exists as an oligomer. Initial crystallization experiments proved fruitless, so GADD45 β was re-cloned in two alternative expression vectors with either a His6 or GST tag and there appeared no further problems of oligomerization. The recombinant construct pGEX6P-GADD45 β , which allows expression of the protein as a GST-fusion product containing a highly specific cleavage site for PreScission Protease upstream of the GADD protein, was finally selected. The recombinant protein obtained after GST removal had the sequence reported in Fig. 1. The applied overexpression system was quite efficient, producing more than 6 mg of highly purified protein from 1L of induced culture under the reported conditions. The purity of the protein was estimated to be 98% by SDS-Page after Mono Q purification. The same purity level was estimated by analyzing the protein by LC-MS using a C18 or a C4 column and PDA or mass spectrometer to monitor the eluate. The protein was characterized by several techniques, including MW determination of the whole protein and also tryptic fragments obtained upon extensive digestion. The experimental MW was 18096.6 \pm 0.5 Da, in very good agreement with the theoretical value of 18098.3 Da, inclusive of the GPLGS fragment left by PreScission protease cleavage (Fig. 1, underlined) and assuming that all cysteines were in the reduced

state. Trypsin treatment gave rise to all the expected fragments, as identified by molecular weight determination upon LC-MS analysis, all without any inter- or intramolecular bridge. The lack of internally linked cysteines was also confirmed by analyzing the same sample after extensive reduction in 10 mM DTT and observing the same peaks pattern as in non reducing conditions. To further address the presence/absence of internal disulfides, we carried out an extensive alkylation reaction on the purified protein in the absence of any reducing agent, using 4-VP. The resulting product was again analyzed by LC-MS under the reported conditions, showing an increase of MW of 630.8 Da, corresponding to the incorporation of six 4-VP moieties. Data concerning the capacity of GADD45 proteins to oligomerize (Kovalsky et al., 2001) are apparently in contrast with our results which, indeed, show that GADD45 β could be present as a monomer. Gel filtration and native electrophoresis experiments have not yet addressed this point, as some oligomers can be held together by covalent linkages depending only on concentration conditions. The secondary structure of recombinant GADD45 β was investigated by means of CD in the far-UV region. The spectrum of native GADD45 β showed two negative bands at 209 and 219 nm and a positive band at 195 nm. This pattern suggested the presence of a folded structure in solution with a predominantly high α -helical content. To further assess the achievement of the correct folding, we demonstrate that Gadd45 β is able to bind in a dose-dependent fashion a peptide derived by MKK7, a kinase involved in the mechanism, mediated by Gadd itself, of suppression of apoptosis promoted by death receptors (Papa et al., 2004).

*GPLGSTLEELVAC**C**DNAAQKMQTVTAAVEELLVAAQRQDRLLTVGVYESAKLMNVDPDSVVL**C**LLLAIDEEED
DIALQIHFTLIQSF**CC**DNDINIVRVSGMQRLAQLLGEPAETQGTTEARDLH**C**LLVTNPHTDAWKSHGLVEV
ASY**C**EESRGNNQWVPYISLQER*

Figure1: Aminoacidic sequence of recombinant Gadd45 β ; the added N-terminal pentapeptide GPLGS is in italics and underlined; cysteine residues are in bold and underlined.

References

1. De Smaele, E., F. Zazzeroni, et al. (2001). "Induction of gadd45beta by NF-kappaB downregulates pro-apoptotic JNK signalling." *Nature* 414(6861): 308-13.
2. Lu, B., A. F. Ferrandino, et al. (2004). "Gadd45beta is important for perpetuating cognate and inflammatory signals in T cells." *Nat Immunol* 5(1): 38-44.
3. Kovalsky, O., F. D. Lung, et al. (2001). "Oligomerization of human Gadd45a protein." *J Biol Chem* 276(42): 39330-9.
4. Papa S, Zazzeroni F, Bubici C, Jayawardena S, Alvarez K, Matsuda S, Nguyen DU, Pham CG, Nelsbach AH, Melis T, De Smaele E, Tang WJ, D'Adamio L, Franzoso G. Gadd45 beta mediates the NF-kappa B suppression of JNK signalling by targeting MKK7/JNKK2, *Nat Cell Biol.* 2004 Feb;6(2):146-53.